BENEMÉRITA UNIVERSIDAD AUTÓNOMA DE PUEBLA

INSTITUTO DE FÍSICA “LUIS RIVERA TERRAZAS”

“DYNAMICAL ASPECTS OF THERMALIZATION IN ISOLATED SYSTEMS OF INTERACTING BOSE PARTICLES”

TESIS

QUE PARA OBTENER EL GRADO DE

DOCTOR EN CIENCIAS (FÍSICA)

PRESENTA

SAMY MAILOUD SEKKOURI

DIRECTORES DE TESIS

DR. FELIX IZRAILEV MIKHAILOVICH
DR. GIUSEPPE LUCA CELARDO

No. de CVU: 825433

JUNIO DE 2021

Abstract

In this work we investigate the Lieb-Liniger (LL) model belonging to the class of integrable quantum many-body systems solvable with Bethe Ansatz, by considering its statistical properties in the many-body Hilbert space, and comparing the results with Random matrix Theory. The quench dynamics of the truncated model (t-LL) is characterized by an exponential spreading of wave packets in the many-body Hilbert space. This happens when the inter-particle interaction is strong enough, thus resulting in a chaotic structure of the many-body eigenstates considered in the non-interacting basis. The semi-analytical approach used here, allows one to estimate the rate of the exponential growth as well as the relaxation time, after which the thermalization emerges.

The key ingredient parameter in the description of this process is the width Γ of the Local Density of States (LDoS) defined by the initially excited state, the number of particles and the interaction strength. In this thesis we show that apart from the meaning of Γ as the decay rate of survival probability, the width of the LDoS is directly related to the diagonal entropy and the latter can be linked to the thermodynamic entropy of a system equilibrium state emerging after the complete relaxation.

We also address the old and debated question of the statistical properties of integrable quantum systems, through the analysis of the Bethe Ansatz solutions. With the use of both analytical and numerical study we show that the properties of spectra strongly depends on whether the analysis is done on the full energy spectrum or on a single subspace of fixed total total momentum. We show the Poisson distribution occurs only when the total momentum is fixed, for not too large or not too weak interaction strength and for sufficiently high energy values. These results show once more that Poisson statistics cannot be considered as a generic one for interacting many-body integrable systems.

Contents

Chapter 1

Introduction

The problem of thermalization in isolated quantum systems remains a hot topic in the field of modern statistical mechanics. It has been shown since long that thermalization can emerge without the presence of a heat bath, even if the number of interacting particles is small [2–7]. One of the main problems in this field is to establish the conditions under which a given system manifests strong statistical properties, such as the relaxation to equilibrium. Due to a remarkable progress in the study of this and related problems, much is already understood in theoretical and numerical approaches (see [8–12] and references therein) as well as in experimental studies of interacting particles in optical traps [13–18], even if many basic problems still need further intensive efforts.

As was shown in Ref. [19], the mechanism for the onset of statistical behavior for a quantum isolated system is the chaotic structure of the many-body eigenstates in a given basis defined in absence of inter-particle interaction. As for the properties of eigenvalues (such as the Wigner-Dyson type of the nearest-neighbour level spacing distribution), it was shown [20, 21] that they have a little impact on the global statistical properties of the wave packet dynamics.

The concept of chaotic eigenstates originates from Random Matrix Theory (RMT), which was suggested by Wigner in order to explain local properties of energy spectra of heavy nuclei, observed experimentally [22, 23]. Being unable to describe global properties of energy

spectra of complex physical systems, the random matrices turned out to be effective models for the description of the local statistical properties of spectra, that were predicted and later confirmed experimentally to be universal. Since long time, the RMT has served as the theory of quantum chaos with strong chaotic properties.

Next steps in the mathematical study of many-body chaotic systems were performed by taking into account the typical two-body nature of the inter-particle interaction. As a result, a new kind of random matrix model, closer to the physical realm than the RMT and known as the Two-Body Random Interaction (TBRI) model has been invented [24–26]. In contrast with the standard RMT, it depends on additional physical parameters, such as the number of interacting particles and the strength of inter-particle interaction. In these matrices a complete randomness is embedded into the two-body matrix elements, from which the many-body matrix elements are constructed.

A distinctive property of the TBRI matrices (in application to both Fermi and Bose particles) is that they are non-ergodic in the sense that the averaging inside a matrix is not equal to the ensemble averaging, even for a very large matrix size [27]. Moreover, these matrices are banded-like, sparse and non-invariant under rotations so that all their properties are related to a specifically given non-interacting basis. For this reason, rigorous analytical analysis (especially, for a finite number of particles) is strongly restricted and many results can be obtained only numerically.

To date, the TBRI matrices are extensively studied, however, mainly in what concerns the properties of energy spectra and structure of eigenstates (see for instance [27–31] and references therein). As for the related time evolution, a close attention to this problem was recently surged ahead by the increasing interest to the problem of scrambling, understood as the loss of information in the process of equilibration and thermalization. Further progress in random matrix theories was achieved due to remarkable results based on the Sachdev-Ye-Kitaev (SYK) model [32,33], which can be considered as a variant of the TBRI

model (see, for instance, Ref. [34]). The SYK model has attracted much attention in recent years, widely accepted as an effective model for two-dimensional gravity, also in application to black holes [35–37]. For the latter problem, a particular interest has been given to the spreading and disappearing of information in the process of thermalization.

As is known, chaos in classical systems is originated from the exponential sensitivity of motion with respect to small perturbations. As a result, the distance in the phase space between two close trajectories increases, in average, exponentially fast and the rate of such an instability is given by the largest Lyapunov exponent λ. In quantum systems, this mechanism is absent due to the linear nature of the Schrödinger equation. Although for quantum systems with a strongly chaotic classical limit, one can observe a complete correspondence to the classical behavior, the time scale $t \sim 1/\lambda$ on which it happens, was found to be dramatically short due to the fast spreading of the wave function. As a result, the chaotic behavior of quantum observables is suppressed in time.

As for quantum systems without classical limit, even in the presence of strong disordered potentials, observation of exponential instability in the quantum motion was questioned for a long time. However, recent remarkable progresses have led to the discovery of the out-of-time-order correlators (OTOC), which are four-point correlation functions with a specific time ordering. Extensive studies have manifested the effectiveness of the OTOC in application to various physical systems [38–41].

It is widely believed that OTOCs can solve the problem of thermalization, however, this is not obvious since their exponential growth in time is bounded by a time scale which cannot be associated with the complete relaxation to equilibrium [42]. Indeed, typical applications of OTOC are mainly restricted by *local* observables, in contrast with the very point that thermalization is a *global* concept. The situation reminds that which was thoroughly discussed in the early stage of the setting up of the classical chaos theory. Specifically, for some time it was believed that correlation functions should typically manifest an ex-

ponential time decrease. Unexpectedly, it was found later that realistic physical systems, even if strongly chaotic, are typically characterized by a quite slow decrease of correlations. Also, an infinite number of correlations functions can be defined and their time behavior can be in principle very different. Thus, even if serving as a good test for the instability of quantum many-body systems, the direct relevance of the OTOC to the time scale of thermalization remains questionable.

One of the first attempts to relate the OTOC to the long-time dynamics in many-body systems has been performed in Ref [43]. Specifically, it was asked whether OTOC can describe the exponential long-time growth of the effective number N_{pc} of components of the wave function, in the process of a complete equilibration. This number can be estimated via the *participation ratio* provided the many-body eigenstates can be considered as strongly chaotic. An important result of this study is that there are two characteristic time scales, one of which is directly related to the survival probability and can be defined in terms of the Lyapunov exponent, therefore, in terms of the OTOC. However, a complete thermalization is described by the excitation flow along a kind of network created by the many-body states. An application of OTOC to such type of dynamics [43] has shown that N_{pc} can be presented as a set of the OTOCs, each of them describing an excitation on a specific time scale, due to standard perturbation theory. For a finite number of many-body states, this process terminates when all states are excited, which create an energy shell in the Hilbert space (for details see [19]).

Numerical data obtained for the TBRI model with a finite number of bosons occupying a number of single-particle energy levels [1], as well as for models of a finite number of interacting spins-1/2 in a finite length chain [20, 21], clearly demonstrated that, in presence of chaotic eigenstates, the global time behavior of the systems is very similar. One has to note that even if one of the spin models is integrable, with a Poisson-like level spacing distribution, this does not influence the quench dynamics. These results confirm the prediction that for many-

body systems the type of energy level fluctuations is less important than the chaotic structure of the many-body states.

In this thesis we continue the study of the quench dynamics, paying attention to the new question of the relevance between the diagonal entropy related to an initially excited state, and the thermodynamic entropy emerging in the process of thermalization. We show numerically and describe semi-analytically that there is a one-to-one correspondence between them, with some corrections due to the different size between interacting and non-interacting energy spectra. This remarkable result holds both for the TBRI model with finite number of bosons, and for the model originated from the celebrated Lieb-Liniger (LL) model [44–46]. The latter model, which has no random parameters, was proved to be integrable with the use of Bethe ansatz.

The LL model describes one-dimensional (1D) bosons on a circle interacting with a two-body point-like interaction. It belongs to a peculiar class of quantum integrable models solved by the Bethe Ansatz [47, 48]; in particular, it possible to show that it has an infinite number of conserved quantities. Apart from the theoretical interest, this model is important in view of various experiments with atomic gases [49–51]. For a weak inter-particle interaction the LL model can be described in the mean-field (MF) approximation. Contrarily, for a strong interaction, the 1D atomic gas enters the so-called Tonks-Girardeau (TG) regime in which the density of the interacting bosons becomes identical to that of non-interacting fermions (keeping, however, the bosonic symmetry for the wave function) [46]. The crossover from one regime to the other is governed by the ratio n/g between the boson density n and the interaction strength g. The latter constant is inversely proportional to the 1D inter-atomic scattering length and can be experimentally tuned with the use of the Feshbach resonance (see, for example, [65] and references therein). Specifically, the MF regime occurs for $n/g \gg 1$ and the TG regime emerges for $n/g \ll 1$ [46].

In our numerical study we consider a *finite* many-body Hilbert space by fixing the total number of momentum states and the number N of

interacting bosons. This truncated Lieb-Liniger model (t-LL) allows one to correctly obtain both the eigenvalues and many-body eigenstates of the original LL model, in a given range of energy spectrum. This method (truncation of the infinite spectrum) can be considered as the complimentary one to the recently suggested way [52], according to which a finite number of eigenstates involving into the quench dynamics is used.

Chapter 2

In this chapter we provide the theoretical foundations for our studies. We start with a short review over Random Matrix Theory and in particular over Two-Body Random Matrix theory. We discuss how quantum chaos emerge in level statistics and complexity of eigenstates for strong interaction. Then we discuss the problem of thermalization for finite number of particles.

In Part I we will introduce the fundamental background that will form a basis for the rest of this work. In particular, we will discuss how the random matrix models we will consider manifest generic signatures of quantum chaos in level statistics and complexity of eigenstates when the density of the levels is high enough. Then we will derive the effective Hamiltonian using the projection formalism and explain how to incorporate the random matrix models into such a framework to properly describe open quantum systems.

Chapter 3

In this chapter we introduce the model and the approach to the solutions. We derive the Hamiltonian in second quantization, look into the symmetries and introduce the truncated model.

Chapter 4

Here we study the spectrum of Bethe Ansatz Approach. We address the problem of genericity of Poisson distribution for level spacing

distribution of integrable systems. In particular, we show that for well known many-body interacting integrable model studied by Lieb and Liniger, Poisson distribution occurs only for particular interaction strengths and particular energy range.

Chapter 5

We study the truncated Lieb-Liniger (t-LL) model by considering its statistical properties in the many-body Hilbert space. We demonstrate that, for a fixed total momentum, the properties of both energy spectra fluctuations and many-body eigenstates follow the predictions of the random matrix theory. Specifically, the level spacing distribution manifests the crossover from the Poisson to the Wigner-Dyson statistics. In the latter situation, the many-body eigenstates can be treated as fully random, in spite of a deterministic nature of matrix elements. By studying the quench dynamics of an initially excited state of the unperturbed Hamiltonian, we have discovered a remarkable relation between the thermodynamic entropy emerging after the relaxation of the system to equilibrium, and the diagonal entropy related to the initial state. Our semi-analytical predictions of the onset of thermalization in the t-LL model are fully confirmed by numerical data.

Part I

Fundamental Concepts

Chapter 2

Quantum Chaos

Initially, the study of quantum chaos was restricted to models of a single particle interacting with external fields. As a result of extensive studies, currently the theory of one-body chaos is developed in great details (see for example, [73–76] and references therein). On the other hand, many problems of many-body chaos occurring in quantum systems of interacting particles are not resolved yet. Recently, the burst of interest in many-body chaos has been triggered by the remarkable progress in experimental studies of trapped systems of bosons and fermions [77] and large-scale exact diagonalization of Hamiltonian matrices for systems of interacting particles.

2.1 Random Matrix Theory

In the first attempt to establish the relation between statistical properties of complex quantum systems and random matrix models [78–81], Lane, Thomas and Wigner introduced an ensemble of banded matrices for the description of conservative systems like atomic nuclei [82]. Assuming time-reversal invariant dynamics, an ensemble of real symmetric infinite Hamiltonian matrices was considered:

$$H_{nm} = \epsilon_n \delta_{nm} + V_{nm} \tag{2.1}$$

The diagonal part was modeled with an equidistant spectrum ("picket

fence"), $\epsilon_{n+1} - \epsilon_n = 1/\rho_0$ where ρ_0 is the level density of the "unperturbed" Hamiltonian $H_0 = \epsilon_n \delta_{nm}$. In Refs. [78–81] the absolute values of the off-diagonal matrix elements were taken equal, $V_{nm} = \pm v$, while the signs were assumed to be random and statistically independent within the band of width 2b around the main diagonal. In a more general case thoroughly studied in Ref. [83], the diagonal elements ϵ_n are random entries, the matrix elements V_{nm} are distributed randomly with $< V_{nm} >= 0$ and $< V_{nm}^2 >= v^2$ for $|m - n| < b$, while $V_{nm} = 0$ outside the band (here and below the angular brackets stand for the ensemble average). The assumption of random character of the "perturbation" V was a pioneering step in the statistical description of complex quantum systems. In his seminal paper of 1955, Wigner wrote that the considered quantum-mechanical systems "are assumed to be so complicated that statistical consideration can be applied to them".

Two important features of the BRM should be stressed. The first point is that the band-like appearance of a matrix is not invariant with respect to orthogonal transformations of the basis. The special basis diagonalizing H_0 should be thought of as corresponding to the mean-field representation. In this way it is assumed the existence of a physically singled out basis in which the treatment of the total Hamiltonian is preferential.

The second point is that the banded structure reflects a finite range of interaction in the energy representation that may emerge from the physical selection rules.

After Wigner's pioneering work, the BRM were almost forgotten (curiously enough, by Wigner himself [78–81]), apparently because of their mathematical inconvenience, namely the absence of invariance with respect to basis rotations. Due to this, attention was paid mainly to full random matrices for which a fairly complete mathematical analysis has been developed [26, 84, 85]. However, in real physical applications full random Hamiltonian matrices can be only used to describe the local statistical properties of spectra and not the global ones. For this reason, such matrices were criticized by Dyson [23] because of the

"unphysical" semicircle law of the total level density.

2.1.1 Two-Body Random Interaction

In order to use the random matrix approach with a more realistic level density, an ensemble of random matrices was suggested in Refs. [24, 25, 86, 87] that takes into account the n-body nature of interaction between the particles (for details and other references, see [26]). Since in the majority of physical applications the main contribution is due to two-body interactions ($n = 2$), this kind of random matrices, known as two-body random interaction (TBRI) matrices, has been studied in great detail. The ensemble of such matrices, referred to as the two-body random ensemble (TBRE), is defined in the secondary quantized form as

$$H = \sum_{p} \epsilon_p a_p^\dagger a_p + \frac{c}{L} \sum_{p,q,r,s} V_{p,q,r,s} a_p^\dagger a_q^\dagger a_r a_s \tag{2.2}$$

Here the term $H_0 = \sum_p \epsilon_p a_p^\dagger a_p$ corresponds to non-interacting particles and $V = \frac{c}{L} \sum_{p,q,r,s} V_{p,q,r,s} a_p^\dagger a_q^\dagger a_r a_s$ absorbs the two-body interaction, where c is the strength of the interatomic coupling interaction, inversely proportional to the 1D interatomic scattering length, and L is the length of the ring. In a more general context, H_0 can be treated as a regular one-body part of the total Hamiltonian written in the mean-field basis, and V represents the residual interaction which, due to its very complicated structure cannot be embedded into the mean field. The entries ϵ_p represent single-particle (or quasi-particle) energies corresponding to single-particle states $|p>$, while $a_p^\dagger$ and a_p are particle creation and annihilation operators for fermions or bosons. These operators define the many-particle basis $|\{p\}_k >= a_{p_1}^\dagger ... a_{p_N}^\dagger |0>$— of non-interacting particles. In this basis H_0 is diagonal with eigenvalues $E_k = \sum_n \epsilon_{p_n}$ defined by the single-particle levels occupied in the many-body state $|\{p\}$. The matrix elements $V_{p,q,r,s}$ of the perturbation V describe a two-body process with indices p, q, r, s indicating initial (r, s) and final (p, q) single-particle states connected by this interaction.

In the TBRI model all matrix elements $V_{p,q,r,s}$ are assumed to be random independent variables. However, due to the two-body nature of the interaction the matrix $H_{k,k'}$ turns out to be band-like, with many vanishing elements inside the band, many non-vanishing matrix elements turn out to be correlated, even in the case of complete randomness of the interaction matrix elements $V_{p,q,r,s}$. As shown in Ref. [59], this is important when analysing the statistical properties of some observables. Apart from the sparsity and intrinsic correlations in TBRI matrices, another difference from the Wigner BRM with the sharp band boundary is that the amplitudes of the matrix elements $H_{k,k'}$ decrease smoothly away from the diagonal. It should be stressed that all these peculiarities are quite typical for physical systems such as complex atoms and nuclei (see, for example, [72, 88])

Quite specific properties emerge if the Hamiltonian reveals additional symmetries so that the Hilbert space can be decomposed into separate subspaces of states, and the dynamics within each subspace is either regular or chaotic.

An unusual result was observed in a simple simulation [89] for few fermions occupying a single level with a large total angular momentum quantum number j and interacting through all types of two-body matrix elements of random magnitude but restricted by rotational invariance. The new aspect here is the interrelation between non overlapping classes of states due to the dynamics driven by the same Hamiltonian. The unexpected result is a clear predominance of ground states of total spin $J = 0$. Statistical considerations [90] qualitatively explain this by assuming that the wave functions are randomized and prefer maximal or minimal values of total spin (precursor of ferromagnetic or antiferromagnetic order). It is interesting that the observed effect seems to be different from the spin glass system [91], where the ground state spin on average grows as the square root of the number N_p of interacting spins. Other regular collective effects also appear with significant probability in such systems with random interactions [92, 93], where a quantitative theory is still absent. One can also use random interac-

tions in order to study possible landscapes arising in the sectors with different values of random parameters. This was done in the interacting boson models [94], where it was possible to delineate the parameter space areas corresponding to different symmetries of the system, and in the nuclear shell model [92], where the random interactions allowed one to find out the sectors of the random parameter space responsible for the predominance of prolate deformation of the mean field.

2.2 Main observables

The problem of quantum chaos was initially referred to one-body quantum systems, fully deterministic but with strong chaos in the classical limit. As was discovered numerically, the properties of such quantum models as the kicked rotor [95–97] and fully chaotic billiards [26, 69, 98, 99] strongly depend on whether the motion is regular or chaotic in the corresponding classical counterparts. It was understood that, unlike classical chaos that is due to the local instability of motion, in quantum chaotic systems the properties of spectra and eigenfunctions have to be compared with those described by full random matrices. It was argued [100, 101] that for integrable systems the nearest level spacing distribution $P(s)$ is generically quite close to the Poisson distribution emerging as a result of absence of correlations between eigenvalues (see also discussion and references in Ref. [97]).

2.2.1 Spacing statistics

In the mid 50s a large number of experiments with heavy nuclei was performed. Heavy many-electron atoms absorb and emit thousands of frequencies. These large systems are typically non-integrable, so solving the eigenvalue problem is impossible. Wigner and Dyson were the first to attack the problem through a statistical point of view. Instead of searching an approximate solution for the nuclear system, they focused on the distribution of energy levels.

"The statistical theory will not predict the detailed sequence of levels in any one nucleus, but it will describe the general appearance and the degree of irregularity of the level structure, that is expected to occur in any nucleus which is too complicated to be understood in detail.." -Freeman J. Dyson

Level spacing distribution

Exponentially fast dynamics in the Fock space of chaotic many-body systems

Spectra of time-reversal systems whose classical analogues are K systems (strongly chaotic) show the same fluctuation properties as predicted by GOE (Gaussian Orthogonal Ensamble), which means that for integrable models the eigenvalues are uncorrelated, and prohibited from crossing and usually their spacings follow the Poisson statistics, In chaotic models the spacings between eigenvalues follow instead the Wigner-Dyson statistics for GOE:

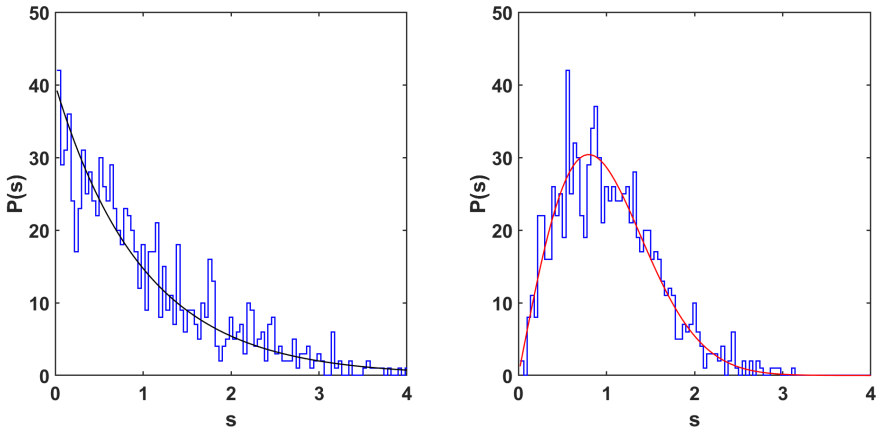

Figure 2.1: Example of the level spacing distribution done with Random Energies and Random GOE matrix compared with Poisson and Wigner distributions respectively.

For a long time the numerical check whether the form of $P(s)$ is close to the Wigner-Dyson distribution has served as the main tool for

the characterization of quantum chaos.

Ratio of consecutive level spacings

Recent papers [119] show how the ratio of consecutive level spacings can be used to analyze the repulsion between levels. This procedure has the advantage of not requiring the unfolding of the spectrum. In practice, following Ref. [119] we introduce the variable

$$\xi_n = \frac{s_n}{s_{n-1}} \quad , \quad s_n = E_n - E_{n-1} \tag{2.3}$$

and from that the variable

$$\chi_n = \quad Min(\xi_n,\ 1/\xi_n) \tag{2.4}$$

In Ref. [119] an exact numerical value has been obtained for the average value $\langle \chi_n \rangle = 0.386$ in case of a Poisson distribution for the NNLS .

Δ_3 statistics

To analyze the fluctuation properties, the spectrum has to be unfolded, i.e. the system specific mean level density must be removed from the data. We use the standard approach, see for instance [120], that we briefly summarize here. Let us introduce the function,

$$\eta(E) = \sum_{n=1}^{N} \Theta(E - E_n) \tag{2.5}$$

This function counts the number of levels with energy less than or equal to E and is usually referred to as the staircase function. It is decomposed into a smooth part and a fluctuating part, through the unfolding we can remove the smooth part.

The unfolding consists in mapping the sequence $\{E_1, E_2, ..., E_N\}$ onto the numbers $\{\xi_1, \xi_2, ..., \xi_N\}$ in such a way that the function $\xi(E)$ is the smooth part of $\eta(E)$ and $\hat{\eta}_{fl}(E)$ is the fluctuating part: $\eta(E) = \xi(E) + \hat{\eta}_{fl}(E)$.

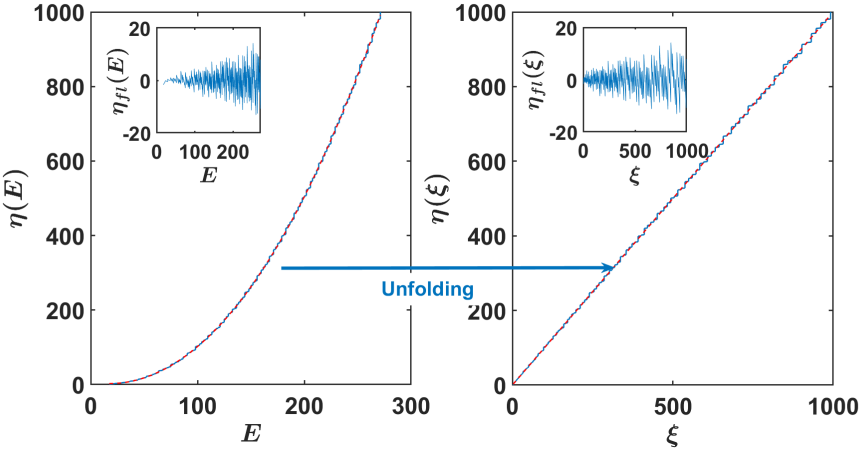

Figure 2.2: Example of the unfolding procedure done with the first exact 300 Bethe Ansatz energies for $N = 5$ particles, $P = 2$ total momentum and strong interaction $n/c = 0.01$. Inset: fluctuating part $\hat{\eta}_{fl}$.

Then we define,

$$\Delta_3 = min_{A,B} \frac{1}{L} \int_{\xi_s}^{\xi_s+L} [\hat{\eta}(\xi) - A\xi - B]^2 d\xi \tag{2.6}$$

where $\hat{\eta}(E)$ counts the number of levels in the interval $[\xi_s, \xi_s + L]$.

Minimizing (2.6) we obtain:

$$\begin{cases} \frac{d\Delta_3}{dA} = -\frac{2}{L} \int_{\xi_s}^{\xi_s+L} \xi[\hat{\eta}(\xi) - A\xi - B] d\xi = 0 \\ \frac{d\Delta_3}{dB} = -\frac{2}{L} \int_{\xi_s}^{\xi_s+L} [\hat{\eta}(\xi) - A\xi - B] d\xi = 0 \end{cases} \tag{2.7}$$

whose solutions,

$$\begin{cases} A = \dfrac{px_1 - 2q}{x_1^2 - 2x_2} \\ B = \dfrac{qx_1 - px_2}{x_1^2 - 2x_2} \end{cases} \tag{2.8}$$

are given in terms of the following quantities

$$x_1 = \frac{2}{L} \int_{\xi_s}^{\xi_s+L} \xi d\xi = 2\xi_s + L \tag{2.9}$$

$$x_2 = \frac{2}{L} \int_{\xi_s}^{\xi_s+L} \xi^2 d\xi = \frac{2}{3}(L^2 3\xi_s^2 + 3\xi_s L) \tag{2.10}$$

$$p = \frac{2}{L}\int_{\xi_s}^{\xi_s+L} \hat{\eta}(\xi)d\xi \tag{2.11}$$

$$q = \frac{2}{L}\int_{\xi_s}^{\xi_s+L} \xi\hat{\eta}(\xi)d\xi \tag{2.12}$$

$$t = \frac{2}{L}\int_{\xi_s}^{\xi_s+L} \hat{\eta}^2(\xi)d\xi \tag{2.13}$$

from them Δ_3 follows easily,

$$\Delta_3 = \frac{1}{2}t + \frac{1}{2}A^2x_2 + B^2 - Aq - Bp + ABx_1 \tag{2.14}$$

2.2.2 Chaotic Eigenstates

It is understood now that the level spacing distribution $P(s)$, although serving as a common test for distinguishing between integrable and non-integrable models, is not effective in application to many-body chaos. First, this quantity that requires precise knowledge of relatively long consecutive series of energy levels of fixed symmetry often is far from being experimentally accessible. Second, the level spacing statistics is typically a weak characteristic of quantum chaos that appears already in the first stages of the process of chaotization. Third, the presence or absence of the Wigner-Dyson level spacing distribution cannot be a necessary condition for classical chaos: for instance, a transition from the Poisson to Wigner-Dyson distribution was found in Ref. [103] in the energy spectrum of the Bunimovich billiard, which is known to be fully chaotic. Finally, in many realistic systems the behavior of various observables is not directly related to the spectral statistics and continues to evolve with the strength of the perturbation after the function $P(s)$ has been stabilized.

On the other hand, it was also numerically observed [98] that the eigenfunctions of the stadium billiard have a quite complicated structure in the position representation. These results have led to the conjecture that the eigenstates of chaotic billiards may be compared to plane

waves with random amplitudes [102]. Later, the complex structures of eigenstates were confirmed for many autonomous systems, as well as for time-dependent systems with external periodic perturbations (for references, see, for example, [97]).

In this situation the knowledge of the structure of the eigenstates turns out to be decisive in understanding regular or chaotic properties of realistic systems. In what follows, we define quantum chaos in terms of the (chaotic) structure of eigenstates, rather than in terms of the level statistics. This idea of shifting the definition of chaos onto individual eigenstates, rather than just on the spectral statistics, has been exploited in Ref. [104]. Specifically, it was suggested to define quantum chaos occurring in an individual eigenstate by the vanishing correlation function between the eigenstate components in an appropriate basis.

In Ref. [105] the emergence of chaotic eigenstates was found when analyzing experimental data for the rare-earth cerium atom. It was shown that excited eigenstates of four valence electrons with the total angular momentum and parity $J^{\Pi} = 1^{+}$ are random superpositions of a number of basic states. Although this number was found to be relatively small as compared with chaotic eigenstates in heavy nuclei [106], one can speak about chaotic atomic states. Later on, intensive analytical and numerical studies [88] have confirmed the onset of chaos in both eigenstates and spectrum of the cerium atom. With the use of the relativistic configuration-interaction method it was shown that the structure of eigenstates of odd and even levels of this atom with angular momentum $J = 4$ above $1eV$ excitation energy becomes similar to that of compound states in heavy nuclei. It was found that the atomic stationary states are random superpositions of about $N_{p.c.} \sim 100$ components built of the $4f, 6s, 5d$ and $6p$ single-electron orbitals. Thus, even four interacting electrons in the mean field of an inert core create chaotic eigenstates. The eigenstates of the random matrix model are qualitatively the same as those of the real atom with no random parameters. These data demonstrate that the TBRI model can effectively describe generic properties of realistic physical systems which are

completely deterministic.

2.2.3 Thermalization

As discussed above, in many physical situations the eigenstates of an isolated system of interacting particles can be treated as chaotic superpositions of their components in an appropriate many-particle basis. This fact has been used in Ref. [59, 88, 107–109] for developing the statistical approach to the description of various observables, based on two key ingredients, the notion of the strength function and the shape of eigenstates in the basis of non interacting particles (or quasi-particles). In this way a natural question arises about the possibility of thermalization in isolated systems in spite of the absence of a heat bath. In the canonical description of conventional statistical mechanics, thermalization is directly related to the temperature defined by the heat bath; any definition of temperature (for example, through the kinetic energy of an individual particle, statistical canonical distribution, or via the density of states) gives the same result. Contrary to that, in isolated systems of a finite number of particles, these temperatures can be different, and the difference increases with the decrease of the particle number. This is also known for classical systems; the detailed study of different temperatures has been done for interacting classical spins moving on a ring [58]. With an increase of the particle number N, all definitions of temperature tend to the unique value, corresponding to the standard result of the thermodynamic limit $N \to \infty$. In this limit (both in classical and quantum mechanics), the statistical behavior of systems emerges irrespectively of whether the system under consideration is integrable or non-integrable, (see, for example, Refs. [110–114]).

Thus, the definition of "thermalization" in application to isolated mesoscopic systems is obscure; for this reason we prefer to speak of thermalization in a broader context, namely, as the existence of statistical relaxation to a steady state distribution. As rigorously shown in Refs. [110, 115], in the thermodynamic limit $N \to \infty$ even for a

completely integrable system an infinitely small subsystem (probe) exhibits statistical relaxation, e.g. the emergence of the Gibbs distribution. With the motion not even ergodic, one can wonder how statistical relaxation can occur since this requires mixing. In the system considered by Bogoliubov this is explained by a perturbation spectrum of the probe oscillator that becomes continuous in the limit $N \to \infty$, a condition necessary for mixing (see discussion in [114]). For finite $N \gg 1$ the spectrum is discrete which implies a quasi-periodic behavior for any observable. However, the characteristic time for revivals is typically so large that on a finite time scale (which, however, could be larger than the lifetime of the Universe) a perfect relaxation occurs. In this sense, quantum chaos can be considered as "temporary chaos", however, indistinguishable from that occurring in classical mechanics on a finite time scale.

A new situation emerges for isolated systems consisting of a finite number of particles. Although in this case the energy spectrum is discrete, the behavior of a system can reveal strong statistical properties, and the adequate theory is based on the notion of quantum chaos. First of all, such a theory has to give an answer to the basic question: when (or under which conditions) the statistical description is possible and practically useful for a quantum isolated system. To answer this question one has to know the mechanism responsible for the onset of statistical behavior. In classical mechanics this problem was solved by the concept of local instability of motion leading to chaotic behavior in spite of completely deterministic equations of motion. In quantum mechanics the Schrödinger equation is linear which means absence of local instability for the time-dependent wave function. For this reason, the chaos that emerges in quantum systems was termed "linear chaos" by Chirikov [116], in order to stress the principal difference from deterministic chaos occurring in non-linear classical systems.

The situation is somewhat easier when a quantum system has a well defined classical limit and the corresponding classical motion is strongly chaotic. Such a situation was originally referred to as "quan-

tum chaos", the term that is nowadays used in other applications such as optics, acoustics, etc. In contrast to classical mechanics, the description of a quantum system is based on the energy spectrum of stationary eigenstates, so that the emergence of quantum chaos in a closed system has to be quantified in corresponding terms. This allows one to speak of quantum chaos in a more general context, namely, including either systems without a classical limit or disordered systems, in contrast with deterministic ones.

As argued in Refs. [3, 5, 109], for an isolated system of a finite number of particles (that can be quite small), the mechanism of thermalization is due to the interaction between particles. When the interaction strength exceeds some critical value, or the level density becomes sufficiently high, the many-body wave functions become extremely complicated ("chaotic") and this leads to thermalization. In a broad sense, this is understood as emergence of relaxation to a steady-state distribution allowing for a statistical description. In fact, at such complexity of stationary eigenfunctions expressed in the appropriate basis, the statistical description seems to be the only one reasonable. A direct link between chaotic eigenstates and the conventional statistical distributions (Boltzman, Fermi-Dirac and Bose-Einstein ones) was analytically established in Ref. [117] for the billiard models. Concerning the conditions for the onset of many-body thermalization due to the inter-particle interaction, the basic ideas and their implications were reported in Refs. [109, 118] demonstrating that the role of a heat bath is played by a sufficiently strong interaction between particles.

Chapter 3

Lieb Liniger Model

In order to address these questions we analyze in this thesis a completely solvable 1D interacting Bose gas : the Lieb-Liniger model [46, 63]. It describes a system of N indistinguishable bosons subject to a δ-function pairwise inter-particle interaction potential in a circle with length L. It belongs to the class of quantum integrable models solvable via Bethe ansatz [47, 48].

This model has been widely discussed in literature and in many experiments [64] where atomic gases has been constrained to 1D geometries. At low temperatures, low linear densities, and strong repulsive effective interactions, these 1D atomic gases enter the so-called Tonks-Girardeau (TG) regime [65], described by the $1D$ solvable model of bosons with "impenetrable core" repulsive interactions. In particular, in the TG regime the momentum distribution after many collisions does not relax to the thermodynamic equilibrium given by statistical mechanics [66]. The TG regime, which occur when the ratio between the boson density $n = N/L$ and the inter-atomic coupling constant c (inversely proportional to the 1D inter-atomic scattering length [65]) becomes very small coincides with the onset of fermionization. Physically it means that the density of the interacting bosons becomes identical to that of non interacting fermions (preserving the bosonic symmetry of the wave function). The opposite limit, $n/c \gg 1$ describes a system of weakly interacting bosons and it is called mean-field approximation

(MF). The transition from TG to MF from the point of view of the dynamics in the many-body Hilbert space has been studied in [67].

The Hamiltonian of our system, composed of N bosons in a ring with length L is given by ($\hbar = 2m = 1$):

$$H = H_0 + V = -\sum_i \frac{\partial^2}{\partial x_i^2} + c\sum_{i\neq j}\delta(x_i - x_j) \tag{3.1}$$

3.1 Second Quantization

Many-body representation is more suited for a comparison with TBRI model. Here the states are represented in Fock basis, which are constructed by filling each single particle state with a certain number of identical particles.

The second quantized Hamiltonian follows from the expectation value of H with the field operators $\psi(x)$.

$$\psi(x) = \frac{1}{\sqrt{L}}\sum_p a_p \exp(ipx)$$

$$\psi^\dagger(x) = \frac{1}{\sqrt{L}}\sum_p a_p^\dagger \exp(ipx) \tag{3.2}$$

the field operator $\psi^\dagger(x)$ acting on the vacuum state creates a particle at position x. The one particle part of it becomes:

$$H_1 = -\int dx \psi^\dagger(x)\frac{\partial^2}{\partial x_i^2}\psi^(x) \tag{3.3}$$

Doing the transformation one can obtain the Hamiltonian in momentum representation

$$H_1 = \sum_p p^2 a_p^\dagger a_p \tag{3.4}$$

The Two particles part of it becomes:

$$H_2 = c\int\int dxdy\psi^\dagger(x)\psi^\dagger(y)\delta(x-y)\psi^(x)\psi^(y) \tag{3.5}$$

Which in moment representation become:

$$H_2 = \frac{c}{L} \sum_{p,q,r,s} a_p^\dagger a_q^\dagger a_r a_s \delta(p+q-r-s) \tag{3.6}$$

3.1.1 Total momentum conservation

As one can see, the Hamiltonian in eq. 3.1 is space invariant ($\{x_i\} \to \{x_i + c\}$), this mean that the the total momentum is conserved. This can be seen also in second quantization, in the δ-function of the interaction matrix, we can see the conservation of the momentum for the created and destroyed particles. Due to this we can reduce the Hilbert space to the one with total momentum of the initial state. Another symmetry that emerge is the reflection ($\{x_i\} \to \{-x_i\}$), which is not a continuous symmetry, therefore it does not lead to a conservation but to the same symmetry in momentum space, as we will show later in Bethe Ansatz approach. To ignore this symmetry we worked on fixed total momentum different from zero.

3.1.2 Truncation

The Lieb-Liniger model is a continuum field theory. The Hilbert space is spanned by infinitely many states, and the Hamiltonian is thus a matrix with infinite dimensions. To proceed, we have to truncate the Hilbert space in some manner to obtain a finite matrix, which can then be diagonalized to obtain the eigenstates and their energies.

As we will show later, due to this truncation we obtain very interesting results different from Bethe Ansatz solutions for strong interactions.

Part II

Results

Chapter 4

Bethe Ansatz approach

Our model belongs to the class of quantum integrable models solvable via Bethe ansatz [47, 48]. This model has been widely discussed in literature and in many experiments [64] where atomic gases has been constrained to 1D geometries. At low temperatures, low linear densities, and strong repulsive effective interactions, these 1D atomic gases enter the so-called Tonks-Girardeau (TG) regime [65] , described by the 1D solvable model of bosons with "impenetrable core" repulsive interactions. In particular, in the TG regime the momentum distribution after many collisions does not relax to the thermodynamic equilibrium given by statistical mechanics [66]. The TG regime, which occur when the ratio between the boson density $n = N/L$ and the inter-atomic coupling constant c (inversely proportional to the 1D inter-atomic scattering length [65]) becomes very small coincides with the onset of fermionization. Physically it means that the density of the interacting bosons becomes identical to that of non interacting fermions (preserving the bosonic symmetry of the wave function). The opposite limit, $n/c \gg 1$ describes a system of weakly interacting bosons and it is called mean-field approximation (MF). The transition from TG to MF from the point of view of the dynamics in the many-body Hilbert space has been studied in [67].

The Hamiltonian of our system, composed of N bosons in a ring

with length L is given by:

$$H = H_0 + cV = -\sum_i \frac{\partial^2}{\partial x_i^2} + c\sum_{i\neq j}\delta(x_i - x_j) \tag{4.1}$$

The solutions for the eigenvalue problem can be obtained through the ansatz wave function, see for instance Refs. [120] and reference therein,

$$\psi(\{x_k\}_\alpha) = \sum_\alpha a(\alpha)\exp[i\sum_{n=1}^{N} x_n\lambda_n^\alpha] \tag{4.2}$$

where: $a(\alpha)$ is the phase factor and λ are called rapidities (quasi-momenta).

Fixing periodic boundary conditions and the ansatz wave function (4.2), one obtains infinite systems of N Bethe equations:

$$\lambda_i^\alpha = \frac{2\pi}{L}m_i^\alpha - \frac{2}{L}\sum_{k\neq i}^{N}\arctan(\frac{\lambda_i^\alpha - \lambda_k^\alpha}{c}) \Rightarrow \quad \begin{cases} \lambda_1^\alpha \\ ... \\ ... \\ \lambda_N^\alpha \end{cases} \tag{4.3}$$

Each combination $\{m_i\}_\alpha$ refers to the eigenstate labelled by α in terms of a set of N "quantum numbers" ($m_i^\alpha \neq m_j^\alpha$) which are integers (half integers) for an odd (even) number of particles N.

The total momentum can be calculated in terms of the rapidities λ_i^α through the Ansatz wave function:

$$\begin{aligned} \hat{P}\psi(\{x_k\}_\alpha) &= \textstyle\sum_j -i\frac{\partial}{\partial x_j}\psi(\{x_k\}_\alpha) = \Big[\sum_j \lambda_j^\alpha\Big]\psi(\{x_k\}_\alpha) \\ &= \Big[\tfrac{2\pi}{L}\textstyle\sum_j m_j^\alpha\Big]\psi(\{x_k\}_\alpha) \end{aligned} \tag{4.4}$$

As for the eigenenergies, they are given by,

$$E_\alpha = \sum_{j=1}^{N}(\lambda_j^\alpha)^2 \tag{4.5}$$

For the following discussion it is interesting to note that there are two simple limit cases:

- infinite interaction, fermionization, free fermions

$$c = \infty, \quad \lambda_j^\alpha = \frac{2\pi}{L} m_j^\alpha \tag{4.6}$$

- no interaction, free bosons

$$c = 0, \quad \lambda_j^\alpha = \frac{2\pi}{L}(m_j^\alpha - j + \frac{N+1}{2}) \tag{4.7}$$

In the following we will set for simplicity $L = 2\pi$ and N odd, so that the rapidities obtained from Eqs.4.6,4.7 are distinct integer numbers. Since the eigenenergy is the sum of N squared distinct integer numbers (see Eq.(4.5)) it is quite clear that the nearest neighbor level spacing distribution cannot be Poisson in the limiting cases $c = 0$ and $c = \infty$. One can wander whether this feature persists also for finite interaction strength and for all energies. We will investigate this feature in the next section, focusing now on the particular characteristics of the energy spectrum.

4.1 Independent spectra

Setting $L = 2\pi$, each eigenstate can be labelled by an integer number (which is the total momentum). Arranging the eigenvalues according to i) its momentum and ii) its growing energy, we obtain for the Hamiltonian an infinite block diagonal structure with each block disconnected from any other (due to momentum conservation there are no matrix elements connecting states with different momenta). In the following we will consider the level statistics in each separate block showing that they are not independent.

In order to prove that let us first start from Eq.(4.3):

$$\lambda_i = m_i + \sum_{k \neq i} f(\lambda_i - \lambda_k), \tag{4.8}$$

with $f(x) \equiv \arctan(x)/\pi = f(-x)$.

Each set of different integers $\{m_i\}_{i=1}^{N}$, determine a set of rapidities λ_i characterizing an eigenstate with energy and momentum,

$$E\{\lambda_i\} = \sum_i \lambda_i^2 \qquad P\{\lambda_i\} = \sum_i \lambda_i \tag{4.9}$$

Let us now consider the shifted set of quantum numbers $m_i' = m_i + k$ with k a positive or negative integer number. It is clear that the shifted rapidities $\lambda_i' = \lambda_i + k$ satisfy the same equations (4.8)

$$\lambda_i' = m_i' + \sum_{k \neq i} f(\lambda_i' - \lambda_k') \tag{4.10}$$

but with momentum and energy given by:

$$P\{\lambda_i'\} = \sum_i (\lambda_i + k) = P + kN \tag{4.11}$$

$$E\{\lambda_i'\} \quad = \textstyle\sum_i (\lambda_i + k)^2 = E\{\lambda_i\} + \nu \tag{4.12}$$

where $\nu = 2kP + k^2 N$ is an integer number.

This means that, since the number of particles N is given, all energies corresponding to a some fixed momentum P, will be shifted by the same constant ν (and thus the levels statistics inside an eigenspace with fixed total momentum will be the same).

In particular, let us note that for $k = -2P/N$ (consider here that only k integer is valid) then $\nu = 0$ and $P\{\lambda_i'\} = -P\{\lambda_i\}$, so we found the well known property that each eigenenergy with $P \neq 0$ is double degenerate.

Let us now analyze in more details Eq.4.11,4.12. Setting for instance $k = 1$ the energy spectrum for P and $P + N$ are simply shifted by the factor $\nu = 2P + N$. This suggests that, at most, only spectra for $P = 0, 1, ...N - 1$ might be independent. But it is not the case. Actually $P = 1$ and $P = N - 1$ have the same spectrum (within a constant shift). To see that simply put $k = 1$ and $P = -1$ in Eq. (4.12 and observe that $P = 1$ and $P = -1$ give the same spectrum. In

the same way $P = 2$ and $P = N - 2$ are the same within a constant shift and so on. The bottom line is that for N odd particles only the spectra for momentum $P = 0, 1, ..., (N-1)/2$, are independent, all the other being simply shifted by a constant. This is a quite unexpected property of the energy spectra since it is completely independent of the interaction strength c.

This simple exercise suggests that much care should be done when computing level statistics since it is well known that computing level statistics without taking into account all the symmetries lead to wrong conclusions. For instance it is well known that Poisson statistics could emerge even superimposing completely independent chaotic spectra (such as those obtained from GOE).

A numerical verification of the simple mathematical proof given above is shown in Fig. 4.1. There we present the firsts 100 levels of $N = 5$ bosons for a fixed value of the interaction $n/c = 1$, solving the Bethe Ansatz equations for different value of total momentum $0 \leq P \leq 9$ and comparing the rescaled energies with the corresponding momenta $P = 0, 1, 2 = (N-1)/2$.

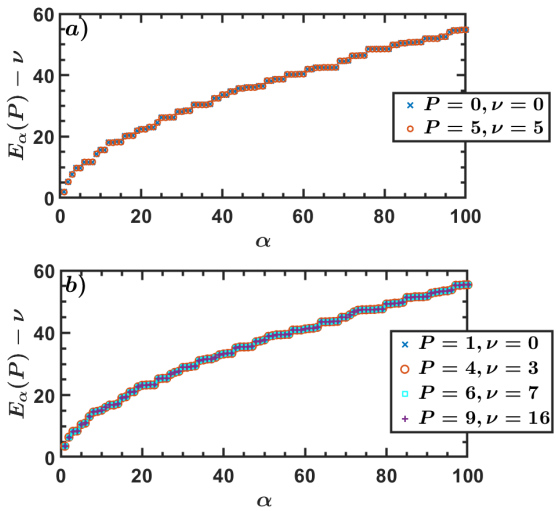

Figure 4.1: (a,b) Firsts 100 energies rescaled by the factor ν with interaction $n/c = 1$ of $N = 5$ particles.

4.2 levels statistics

4.2.1 The limiting cases

As discussed above, for $c = 0$ and $c = \infty$ the eigenenergies are obtained by the sum of N squared integers and thus the NNLS cannot be Poisson. One might wonder if this behavior persists also when $c \ll 1$ or $c \gg 1$. Instead of using a particular interaction strength it is much more significative to use the ratio n/c. In Fig.4.2 we show the NNLS for a weak interaction $n/c = 1$ and for strong interaction $n/c = 0.01$. As one can see: i) the NNLS shows a very pronounced peak at the origin (at variance with the Poisson distribution showed for comparison) and ii) a peculiar similarity between the two cases indicating the symmetric behavior between the two limiting cases.

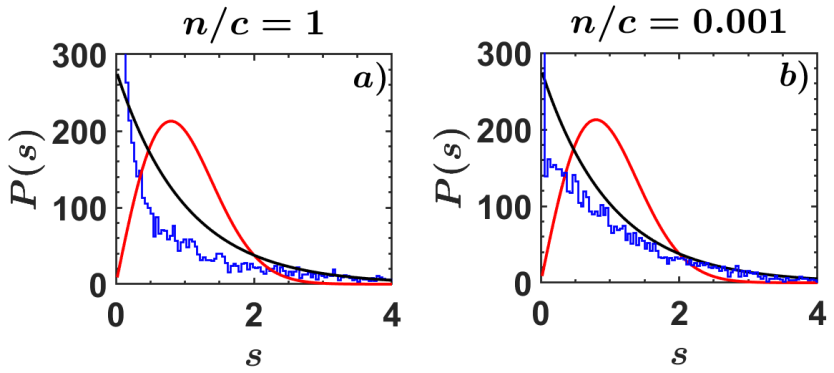

Figure 4.2: NNLS distribution for $N = 5$ particles, momentum $P = 2$ and $n/c = 1$ (a) and $n/c = 0.01$ (b). Black lines indicate the Poisson distribution, red lines the Wigner-Dyson distribution.

Since NNLS does not represent a good tool for searching small deviation we study in the next two sections the Δ_3 statistics, see for example Ref. [120] and reference therein.

4.2.2 Δ_3 statistics

It is well known that in case of a Poisson NNLS $\Delta_3(L) \propto L$, so we study the deviation of our distribution from the straight line. In Fig.4.3 we show the Δ_3 statistics for different $N = 5$ particles and fixed momentum ($P = 0, 1, 2$ from the left to the right column) and different interaction strength $n/c = 1, 0.1, 10$ (from the top to the bottom line). In each panel we show with different color Δ_3 for the same number of energies in different parts of the spectrum, from the lowest (close to the ground state) to the upper part (we computed up to 10^6 eigenvalues and since the spectrum is actually infinite it is meaningless to talk about upper part of the spectrum).

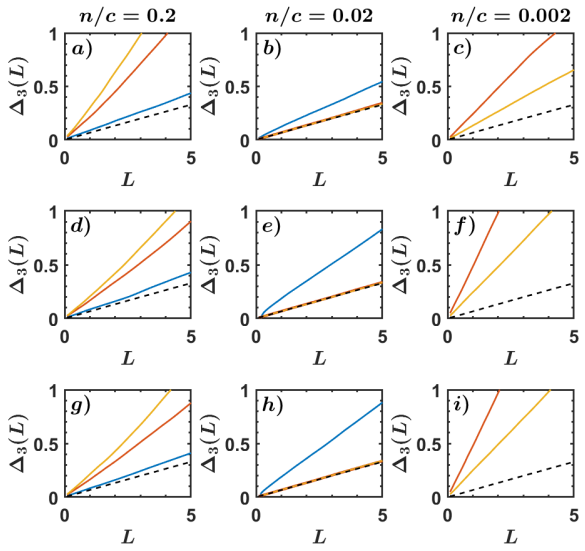

Figure 4.3: Average Δ_3 statistics comparison for different fixed total momentum $P = 0, 1, 2$ (respectively upper , middle and lower row) of 10^4 consecutive initial energies. Each column represent a different interaction strength : left column $n/c = 0.2$, middle column $n/c = 0.02$, right column $n/c = 0.002$. Different colours indicated different energy regions : low energy region with ξ_n starting from $n = 1$ in blue, middle energy region with ξ_n starting from $n = 10^6$ in red and ξ_n starting from $n = 2 \times 10^6$ in purple. Dashed black line stands for Poisson statistics.

As one can see from the comparison with the analytical prediction for the Poisson spectrum only for very strong interaction $n/c = 0.01$ and excluding the lowest part of the spectrum we may speak of Δ_3 statistics close to the predictions given by the Poisson NNLS.

In order to study in a systematic way the deviations from Poisson (straight line) we fit $\Delta_3(L)$ with a line

$$\Delta_3(L) = \gamma_0 L + \gamma_1 \tag{4.13}$$

in the range $0 \leq L \leq 5$ and we plot γ_0 as a function of the interaction strength n/c for different energy ranges in the spectrum (se different symbols in Fig.4.4). As one can see for any energy range one can find a suitable range in the interaction strength (not too weak, not too strong) in which there is good correspondence with a Poisson NNLS.

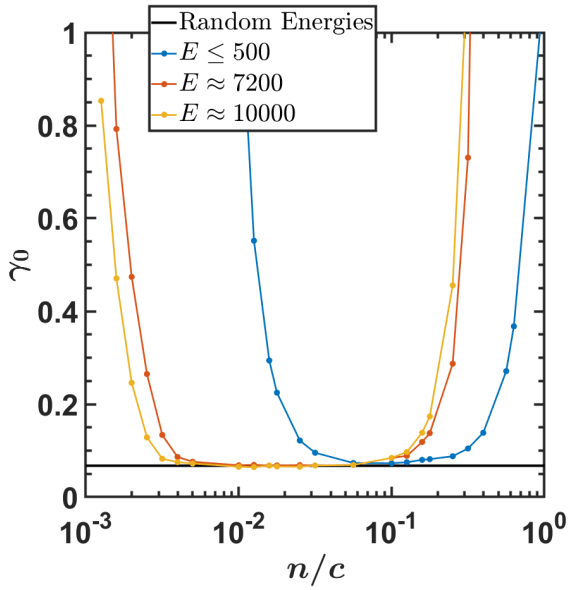

Figure 4.4: Slope of $\Delta_3(L)$ for different value of interaction and location in the spectrum as in previous figures, compared with the slope obtained with Random Energies: black line. Here we choose the $P = 2$ total momentum and the average is done over a set of 10^4 energies around the energy indicated in the legend. The log scale in x-axis also show a nice symmetry around some interaction strength n/c dependent of the chosen energy range.

From this picture it is clear that from one side one can say that for any energy range a suitable value of the interaction can be found in order to have a Δ_3 test indicating similarity with Poisson statistics. The bad is for any interaction strength one can find an energy range where Δ_3 statistics indicates strong deviation from Poisson.

Actually the rigidity of the spectrum (linear straight line with slope 1/15) last for small L values also in the so called Poisson region, as shown in Fig. 4.5. Therefore, a kind of correspondence to Poisson statistics is restricted by nearest levels.

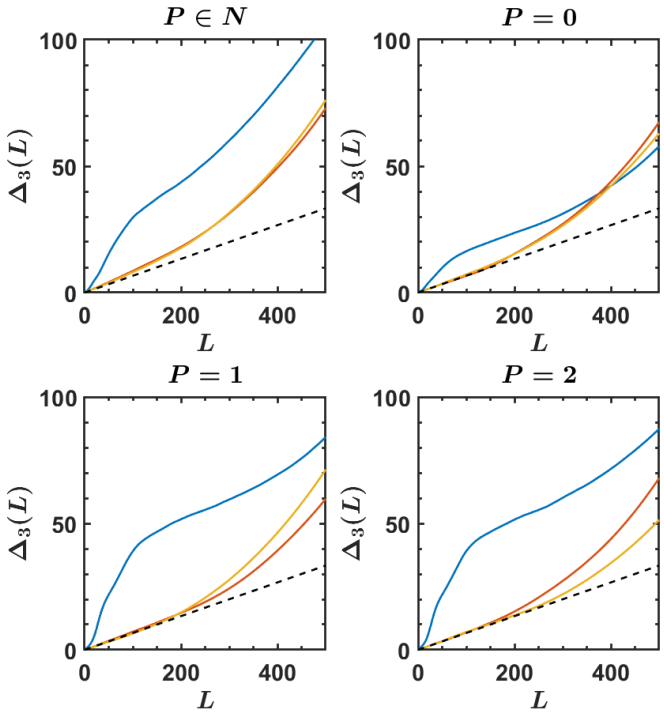

Figure 4.5: Average Δ_3 statistics comparison for large L values. Data are the same as Fig.4.3 central column

4.2.3 Statistics of close energies

In Fig.4.6 we show for different interaction strength n/c, different momentum values and different energy range our numerical results (light blue dots) compared with the theoretical prevision for a Poisson distribution (red line). To facilitate the comparison we average χ_n over 500 consecutive n values (yellow circles) . These results are in agreement with those found with the Δ_3 statistics. Indeed, as one can see, while there is a good agreement with Poisson for large enough energy and interaction $n/c = 0.01$, for small interaction $n/c = 1$ our results shows a strong level clustering with an average value definitely smaller than the Poisson reference.

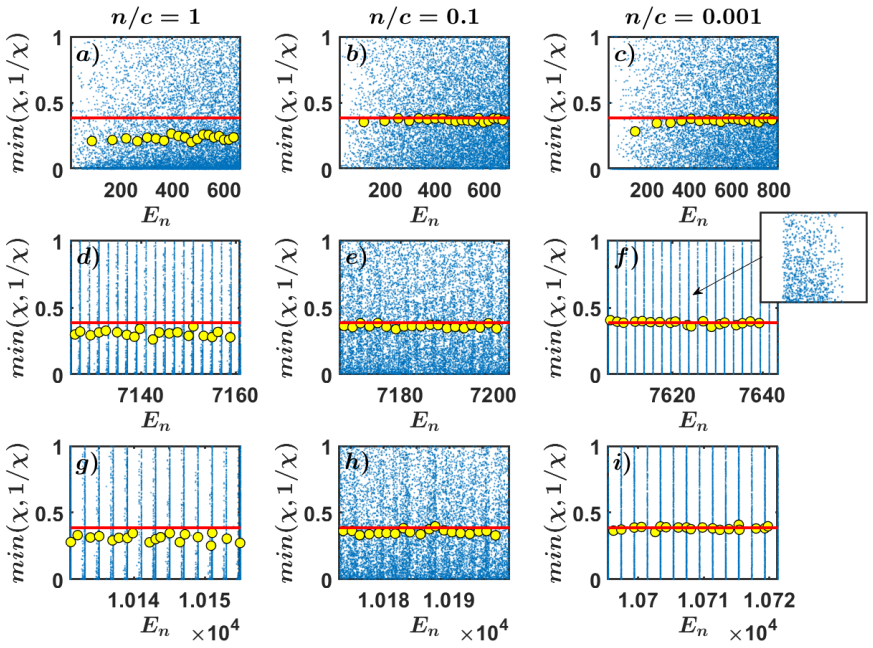

Figure 4.6: Blue dots: 10^4 values of $\min(\chi_n\ ,\ 1/\chi_n)$. Different rows indicates different spots of the energy spectrum (see x-axis), while different columns indicate different values of the interaction strength (as indicated in the legend. Yellow dots are the average over 500 close values while the red continuous line is the value obtained from Random Energies ($y = 0.386$). Parameters are : $N = 5$, $P = 2$.

As a third figure of merit we can compare the distribution functions for the variable χ, $P(/\chi)$. In [119] it has been shown that for a Poisson NNLS one has the normalized distribution

$$P(x) = 1/(1+x)^2. \tag{4.14}$$

In Fig.4.7 we compare the distributions obtained numerically for different interaction $n/c = 1, 0.1, 0.01$, different momenta $P = 0, 1, 2$ and different energy range with Eq.4.14. The strong clustering for weak interaction $n/c = 1$ has been confirmed in a strongly peaked $P(x)$.

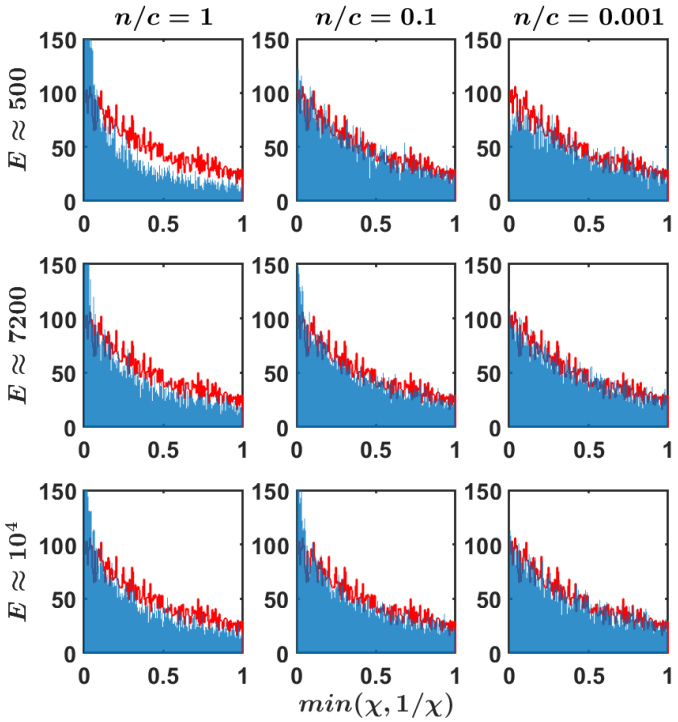

Figure 4.7: Distributions of $\min(\chi_n\ ,\ 1/\chi_n)$, for total momentum $P = 2$ and different interactions (written above) of 10^4 Energies. Red lines: distributions made for 10^4 Random energies. The x-axis is divided in 200 bins.

Chapter 5

Truncated Lieb-Liniger approach

The Hamiltonian of the LL model with N bosons occupying a ring of length L, in momentum representation has the following form (in dimensional units),

$$H = H_0 + V = \sum_k \epsilon_k \hat{n}_k + \frac{g}{2L} \sum_{k,q,p,r} \hat{a}_k^\dagger \hat{a}_q^\dagger \hat{a}_p \hat{a}_r \delta(k+q-p-r). \quad (5.1)$$

Here $\hat{a}_k^\dagger$ and $\hat{a}_k$ are the creation/annihilation operators acting on a single-particle level k of the momentum, and $\hat{n}_k = \hat{a}_k^\dagger \hat{a}_k$ is the number of particles in the the corresponding $k-$level. Thus, the single-particle energy levels (for non-interacting bosons) are given by

$$\epsilon_k = \frac{4\pi^2 k^2}{L^2}. \quad (5.2)$$

The $\delta-$function in space configuration indicates the momentum conservation at the process of the two-body interaction. Below, the single-particle states $|\phi_k\rangle$ are labeled according to their momentum $k = 0, \pm 1, \pm 2, ...$ From them, the many-body unperturbed states $|j\rangle = |...n_{-k}...n_0, ..., n_k...\rangle$ have been built, where n_k indicates the number of particles in the k-th momentum level. In our numerical study, we consider a finite number N of particles occupying $\ell = 2M + 1$ of single-particle momentum states. Note that the total number of

single-particle energies ϵ_k is $M+1$ since the states with momentum $\pm k$ are degenerate. We choose N and M to be approximately the same (analog of a half-filling, typically considered in spin systems). A rough estimate, $n = N/L \sim g$, for the transition from the MF to the TG regime in connection with quantum chaos, is discussed in Ref. [60].

The many-body states $|\alpha\rangle$ of the total Hamiltonian H can be expressed in terms of the eigenstates $|j\rangle$ of the unperturbed part H_0 in the standard way, $|\alpha\rangle = \sum_j C_j^\alpha |j\rangle$ where the components C_j^α can be obtained by exact diagonalization. Due to the two-body character of the interaction, the matrix elements $H_{ij} = \langle i|H|j\rangle$ are non-zero only when the two unperturbed many-body basis states $|i\rangle$ and $|j\rangle$ have single-particle occupations which differ by no more than two units. This means that the Hamiltonian matrix H_{ij} is sparse which is the underlying property of all many-body models with two-body interaction.

If one reorders the diagonal matrix H_0 according to increasing values of the total momentum, its structure takes a diagonal-block form shown in Fig. 5.3. Here, each block corresponds to a particular value of the total momentum. Moreover, if we further reorder the diagonal elements inside the blocks according to the increasing value of the diagonal elements, all the block-matrices are band-like as shown in the inset of Fig. 5.3. Momentum conservation is manifested in the block structure, the number $2M+1$ of the blocks corresponding to the number of different values of the total momentum.

5.1 Hamiltonian Matrix

The many-body states $|\alpha\rangle$ of the total Hamiltonian H can be expressed in terms of the eigenstates $|j\rangle$ of the unperturbed part H_0 in the standard way, $|\alpha\rangle = \sum_j C_j^\alpha |j\rangle$ where the components C_j^α can be obtained by exact diagonalization. Due to the two-body character of the interaction, the matrix elements $H_{ij} = \langle i|H|j\rangle$ are non-zero only when the two unperturbed many-body basis states $|i\rangle$ and $|j\rangle$ have single-particle occupations which differ by no more than two units.

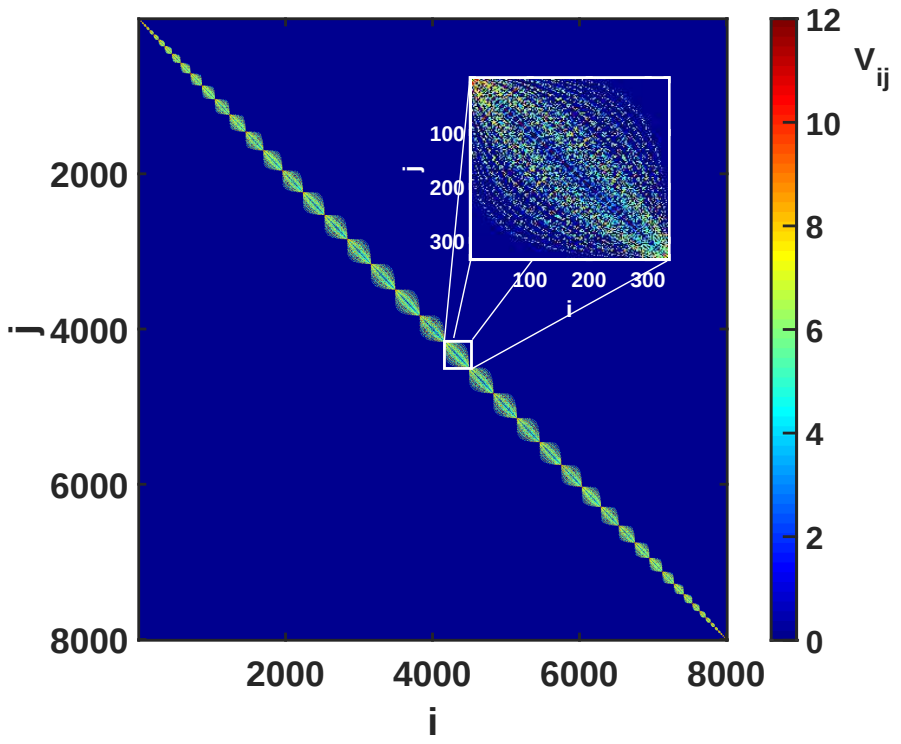

Figure 5.1: Diagonal-block structure of the Hamiltonian matrix for a system with $N = 6$ particles and $\ell = 11$ momentum states. Inset: a single matrix with fixed total momentum $P = 1$ has been singled out. Inside the blocks, the diagonal elements are arranged according to increasing diagonal energies.

This means that the Hamiltonian matrix H_{ij} is sparse which is the underlying property of all many-body models with two-body interaction.

If one reorders the diagonal matrix H_0 according to increasing values of the total momentum, its structure takes a diagonal-block form shown in Fig. 5.1. Here, each block corresponds to a particular value of the total momentum. Moreover, if we further reorder the diagonal elements inside the blocks according to the increasing value of the diagonal elements, all the block-matrices are band-like as shown in the inset of Fig. 5.1. Momentum conservation is manifested in the block structure, the number $2M + 1$ of the blocks corresponding to the number of different values of the total momentum.

5.1.1 Total momentum P=0

As seen in the Bethe Ansatz approach, for total momentum $P = 0$ due to the fact that we have 2 different type of states (symmetric and not-symmetric), the Hilbert space can be divided in two subspaces. Consider the states of the unperturbed Hamiltonian written as $|n_{-M}, n_{-M+1}, ..., n_0, n_1, ..., n_M >$.

1. the subspace for which $n_k = n_{-k}$ for any $k = -M, ..., M$ (symmetric states)

2. the complement of such subspace (the other not-symmetric states). In this subspace each state $|\{n_k\} >$ has his twin degenerate state $|\{n_{-k}\} >$ that has the same diagonal energy since the latter depends on k^2. For each non-symmetric state it is possible to define the symmetric and anti-symmetric states just taking:

$$\frac{1}{\sqrt{2}}(|\{n_k\} > \pm|\{n_{-k}\} >) \tag{5.3}$$

This means that the total Hilbert space is now divided in the two sets of symmetric and antisymmetric states. Since the interaction V is invariant under the change of the momentum signs these two subspaces have no transition amplitudes. In other words we can restrict ourself to the subset of symmetric states only. And this is how the interaction matrix looks like in this new states representation.

For this reason we decided to focus our work on different total momentum sub-spaces, so we don't have to split the matrix again.

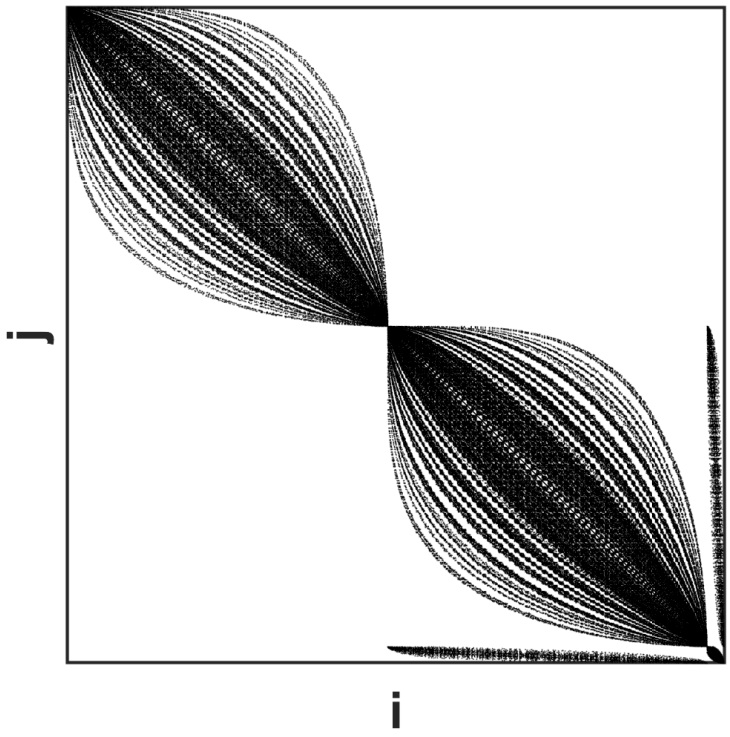

Figure 5.2: Sparsity of $V_{i,j} =< i|V|j >$ for $N = 9$ particles and $l = 13$ states. Here the states $|i > and|j >$ are the symmetric and the anti-symmetric states discussed before. The first block are the anti-symmetric states, the second block are the symmetric states created by two twin degenerate states, and the last small block are the originally symmetric states.

5.2 Total momentum P=1

The structure of the Hamiltonian matrix at some total momentum value M is shown in Fig.5.3 and as one can see it is very similar to the one of TRBI model.

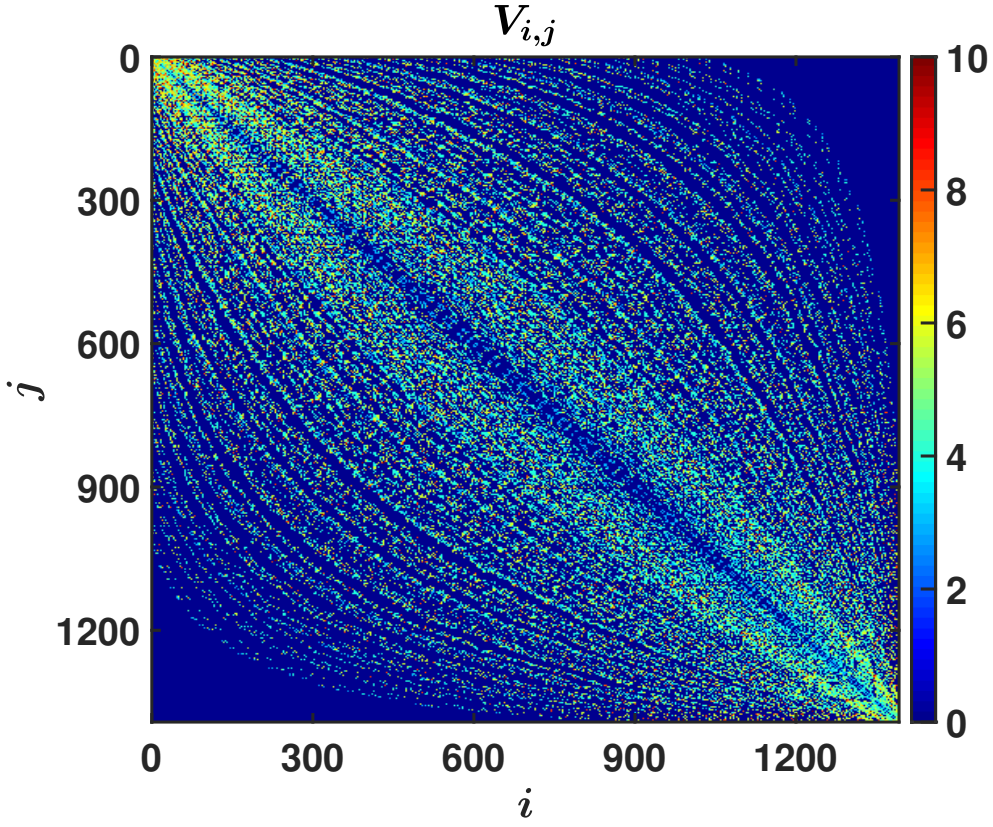

Figure 5.3: t-LL model : Structure of the Hamiltonian matrix for a system with $N = 5$ particles and $\ell = 17$ momentum states and fixed total momentum $P = 1$.

For the case shown in Fig. 5.3 diagonal and off-diagonal Hamiltonian matrix elements take the values from a set with very few elements, as one can see from the plots shown in Fig.5.4. It is important to note that the validity of our analytical expression holds also in this case where the non-interacting density of states is a set of δ-functions (and certainly not a Gaussian).

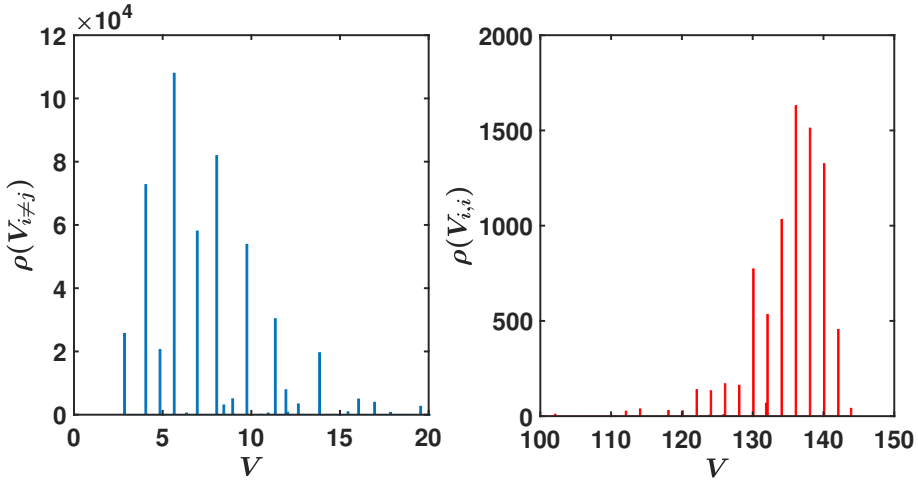

Figure 5.4: Truncated LL model (t-LL). Left panel : distribution of off-diagonal elements $\rho(V_{i,j})$ for the Hamiltonian matrix Eq. Right panel : distribution of diagonal matrix elements $\rho(V_{i,i})$. Here we considered $N = 9$ particles in $\ell = 13$ momentum levels and $g = 1$.

5.3 Level spacing distribution and Eigenstates

One of the standard approaches in the quantum chaos theory is the study of fluctuations of spacings between neighboring energy levels. This approach works fairly good for one-body chaos for which the level spacing distribution $P(s)$ is typically described by famous Wigner-Dyson distribution [68,69]. In the other limit case of integrable Hamiltonian, the form of $P(s)$ is found to be approximately described by the Poisson distribution. In our many-body system, the $P(s)$ is, indeed, close to a Poisson distribution, *if* one considers the spectrum of the total Hamiltonian. This result is due to the absence of correlations between the energy subsets corresponding to different values of the total momentum. Therefore, a non-trivial question is: what type of distribution should be expected for the energy spectrum with a fixed value of the total momentum P only? Below we show, that the answer to this question can be obtained with the use of the two-body *random matrix* ensemble (TBRE), in spite of the fact that our model is not only deterministic (non random) but also completely integrable.

In view of the above question, let us focus on the properties of energy spectra and eigenstates of the LL model, by fixing the total momentum P. To fix ideas, we choose $P = 1$ for which the corresponding matrix is shown in inset of Fig. 5.3. Our main interest is in a strong inter-particle interaction for which we explore the form of $P(s)$ and the structure of eigenstates in connection with the theory of random matrices. Concerning the form of $P(s)$, our extensive data demonstrate a typical transition from the Poisson to the WD distribution on decreasing the key parameter n/g, see Fig. 5.6. The characteristic value for which a clear WD emerges, turns out to correspond to the condition for the crossover from the MF to the TG regime, namely, for $n/g \sim 1$. Such a change in the form of $P(s)$ is quite typical for both disordered and non-disordered quantum systems, when changing the degree of inter-particle interaction [19].

Next, we studied the structure of eigenstates in the middle of the

energy spectrum and found that they are well described by fully random matrices, provided the inter-particle interaction is sufficiently strong. Specifically the RMT predicts that the fluctuations of the amplitudes for these eigenstates follow the Gaussian distribution. The search of this distribution is a very sensitive test for a truly random structure of the eigenstates.

Considering the basis $\{|k>\}$ of the unperturbed Hamiltonian H_0 as our preferential, and the basis $\{|\alpha>\}$ of the total Hamiltonian H

$$H_0|k>=E_k^0|k> \quad , \quad H|\alpha>=E_\alpha|\alpha> \tag{5.4}$$

We can obtain the projection C_k^α by diagonalizing the total Hamiltonian matrix.

$$|\alpha>=\sum_i C_k^\alpha|i> \quad , \quad C_k^\alpha=<i|\alpha> \tag{5.5}$$

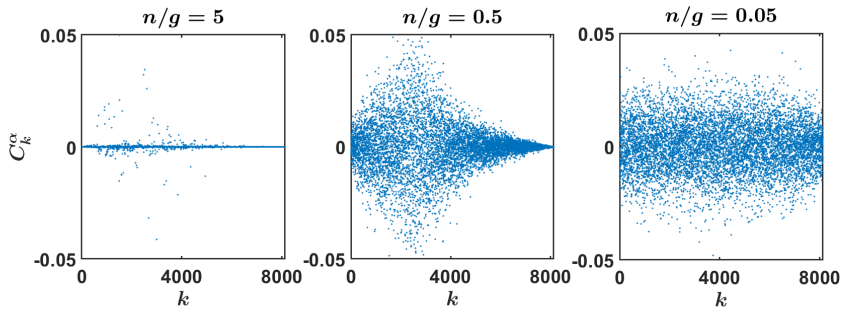

Figure 5.5: Example of one specific Eigenstate in the middle of the spectrum for different values of the interaction strength $n/g = 5, 0.5, 0.05$, written in term of the projections C_k^α, which show a transition to chaos.

Numerical data for the distribution of components of eigenstates is demonstrated in Fig.5.6. One can see an excellent correspondence of the data to the Gaussian distribution $P(C_k^\alpha)$ of the eigenstate components, obtained in the same region of parameters for which the form

of $P(s)$ corresponds to the WD distribution. It is important to stress that in our analysis we have used the statistical χ^2 test for the correspondence of the data to the analytical predictions. For both $P(s)$ and $P(C_k^\alpha)$ this test demonstrates an excellent correspondence to the predictions of the RMT.

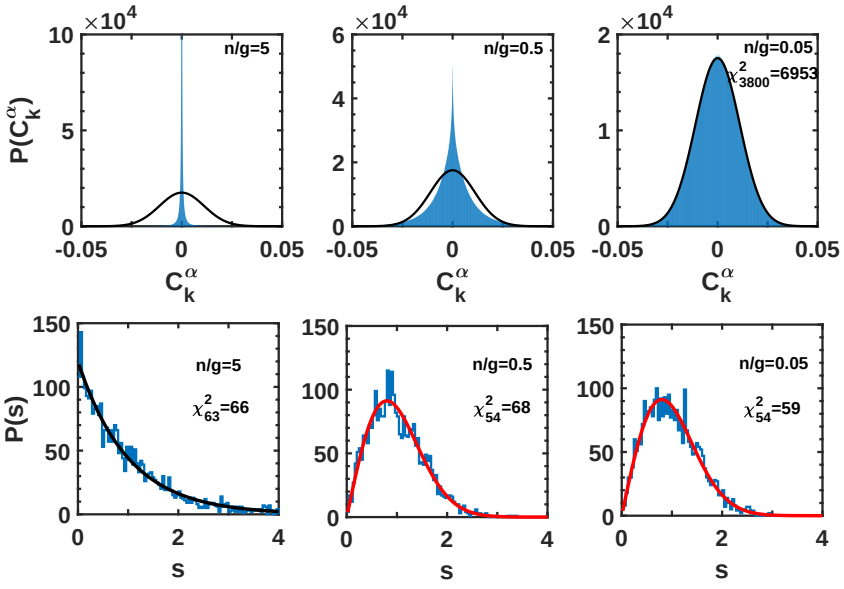

Figure 5.6: First row: The blue bins are Eigenstates components distribution compared with the black line Gaussian distribution $f(x) = A\sqrt{b/\pi}\exp(-bx^2)$ with $b = N_k/2$ ($N_k = 8122$ number of many-body states) of 3001 states in the middle of the energy spectrum $2500 \leq \alpha \leq 5500$ ($A = 3001 \times 8122$). Second row: the blue line is the level spacing distribution compared with both black line Poisson and red line Wigner-Dyson distributions of the same states($2500 \leq \alpha \leq 5500$), for different values of n/g. The χ^2 test (only for bins with more than 50 events for the components distribution and 10 for the level spacing) is shown in the pictures. Here the Components distribution is divided in 5000 bins between $-0.05, 0.05$. While for the level spacing we used 100 bins between $0, 4$. The number of particles is $N = 9$ in $\ell = 2m + 1 = 13$ single particle states, $L = 1$ length of the ring.

5.4 Δ_3 statistics and spacing ratios

As shown above, Δ_3 statistics can discern chaotic systems from integrable ones through Long-range correlations instead of only looking at nearest neighbour.

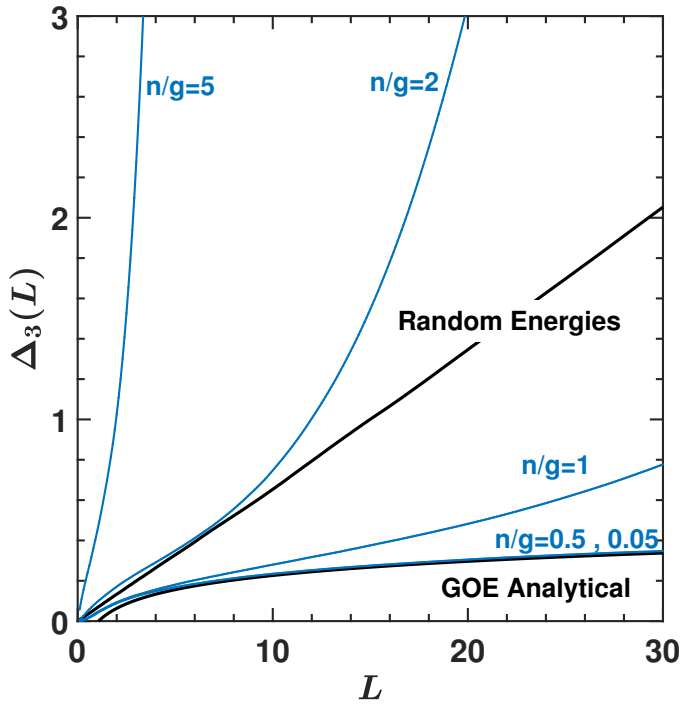

Figure 5.7: Blue lines: Average Δ_3 statistics comparison for different interaction n/g of 5×10^3 energies in the middle of the spectrum. Compared with the one calculated with ordered totally random values and analytical expression of GOE $\Delta_3^{GOE} = \frac{1}{\pi^2}(\ln(2\pi L) + \gamma - \frac{5}{4} - \frac{\pi^2}{8})$.

Figure 5.7 show that increasing the interaction we cross totally uncorrelated energies (Random) around $n/g \approx 1$, and then it reach GOE very fast.

It's also interesting how in the case $n/g = 2$ for short range we have similar behaviour has in Random Energies, but after $L \approx 10$ it starts diverging.

The same study can be done over the ratios of consecutive level spacings. Fig. 5.8 show that the results are consistent with the above, so we won't go into details.

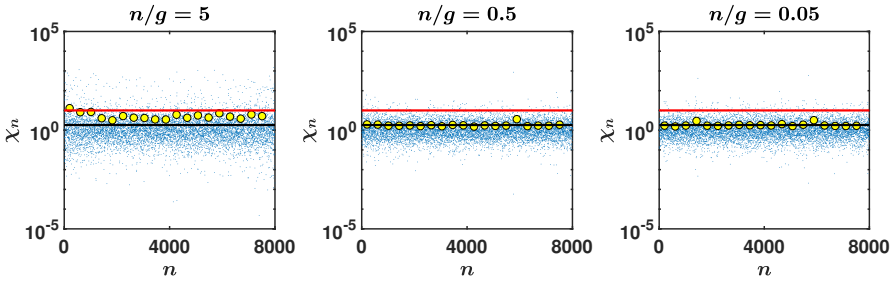

Figure 5.8: Blue dots: Ratios of consecutive levels χ_n for the whole spectrum and different values of the interaction strength, compared with the ones obtained with Random Energies (Red line), GOE random matrix (Black line). Yellow dots: average over 500 values. Parameters: $N = 9$, $P = 1$ and $\ell = 13$.

5.5 Dynamics

5.5.1 Quench dynamics

After specifying the non-interacting basis $|k\rangle$, one can study the wave packet dynamics in this basis, after switching on the two-body interaction V. Our analytical and numerical results refer to the situation when initially the system is prepared in a particular eigenstate of H_0,

$$|k_0\rangle = \sum_\alpha C_{k_0}^\alpha \, |\alpha\rangle \, . \tag{5.6}$$

and evolved according to the full interacting Hamiltonian H. To do this, we focus on the time dependence of the effective number $N_{pc}(t)$ of principal components of the wave function,

$$N_{pc}(t) \equiv \left(\sum_k |\langle k|e^{-iHt}|k_0\rangle|^4 \right)^{-1} , \tag{5.7}$$

known in literature as the *participation ratio*.

In terms of eigenvalues and many-body eigenstates of the Hamiltonian H the participation ratio can be presented as

$$N_{pc}(t) = \left\{ \sum_k \left[P_k^d + P_k^f(t) \right]^2 \right\}^{-1} , \tag{5.8}$$

where

$$P_k^d = \sum_\alpha |C_{k_0}^\alpha|^2 |C_k^\alpha|^2 \tag{5.9}$$

and

$$P_k^f(t) = \sum_{\alpha \neq \beta} C_{k_0}^\alpha C_k^{\alpha *} C_{k_0}^\beta C_k^{\beta *} e^{-i(E^\beta - E^\alpha)t} \tag{5.10}$$

are the diagonal and off-diagonal parts of

$$P_k(t) = |\langle k|e^{-iHt}|k_0\rangle|^2 = \sum_{\alpha,\beta} C_{k_0}^{\alpha *} C_k^\alpha C_{k_0}^\beta C_k^{\beta *} e^{-i(E^\beta - E^\alpha)t}. \tag{5.11}$$

As was recently shown for different models with chaotic behavior [1], the number N_{pc} increases exponentially fast in time, provided the

eigenstates involved in the dynamics, are strongly chaotic. After some relaxation time t_s, the value of N_{pc} fluctuates around the saturation value due to the complete filling of a portion of the total Hilbert space, called energy shell. Such a wave packet dynamics occurs when the many-body eigenstates of H are fully delocalized in the energy shell. This scenario explains the basic properties of the quench dynamics, before and after the saturation.

5.5.2 Semi-analytical approach

The semi-analytical approach developed in [4] for TBRI matrices with an infinite number of interacting Fermi-particles and modified in [1] for finite Bose-systems, allows one to obtain simple estimates for two important characteristics of the quench dynamics. The first characteristic is the rate of the exponential growth for the $N_{pc}(t)$. The second characteristic is the time scale t_s on which the exponential growth of $N_{pc}(t)$ occurs.

The two above characteristics can be estimated with the use of the semi-analytical approach originally developed in [53] for an infinite number of particles. To start with, we write down an infinite set of probability conservation equations, used for the description of the probability flow $W(t)$ in the many-body Hilbert space of H_0. To this end, let us consider an initial non-interacting state $|k_0\rangle$, and the probability $W_0(t)$ to be in this state at the time t. Correspondingly, we define the set $\mathcal{M}_0 = \{|k_0\rangle\}$ consisting of the initial state alone. In order to describe how the probability spreads in time we consider all states $|k_i\rangle$ directly coupled to the initial one via the two-body interaction V. We call this set $\mathcal{M}_1 = \{|k_i\rangle$ for which $|\langle k_0|V|k_i|\rangle \neq 0\}$. From this set we define $W_1(t)$ as the probability to be in $\mathcal{M}_1$ at the time t. As time increases, the probability flows onto another set $\mathcal{M}_2$ (with probability W_2) consisting of those states, coupled with the states of $\mathcal{M}_1$ by non-zero Hamiltonian matrix elements and so on (see Fig.5.9). Neglecting

the backward flow the infinite set of rate equations reads,

$$\begin{aligned} \frac{dW_0}{dt} &= -\Gamma W_0, \\ \frac{dW_1}{dt} &= -\Gamma W_1 + \Gamma W_0, \\ \frac{dW_2}{dt} &= -\Gamma W_2 + \Gamma W_1, \\ &\ldots \end{aligned} \tag{5.12}$$

where we have introduced the parameter Γ describing the exponential decay rate of the initial probability $W_0(t) \equiv P_{k_0}(t)$. In Ref. [53] it was shown that the above equations can be solved exactly:

$$W_k(t) = \frac{(\Gamma t)^k}{k!} W_0(t) \tag{5.13}$$

with $W_0(t) = \exp(-\Gamma t)$. The solution (5.13) allows one to derive the

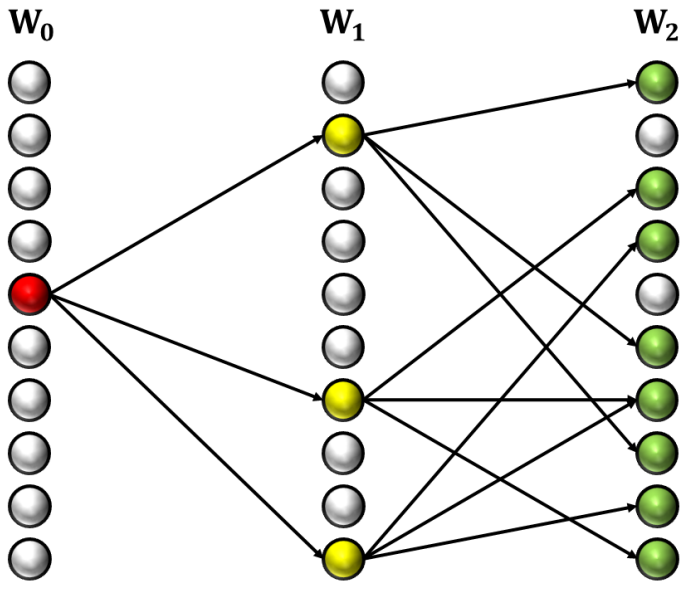

Figure 5.9: Probability flow in the many-body Hilbert space with the connectivity $\mathcal{K} = 3$.

expressions for various observables. Defining the connectivity $\mathcal{K}$ of this

network as the number of the elements in the first set $\mathcal{M}_1$, in [53] the following approximate expression has been obtained,

$$N_{pc}(t) = \exp\left[2\Gamma(1 - \frac{1}{\sqrt{\mathcal{K}}})t\right]. \tag{5.14}$$

It should be stressed that the analogy with an infinitely large "tree" is correct in the thermodynamic limit only. For a finite Hilbert space, as in our case, the number of the effective subsets $\mathcal{M}_k$ is finite. As a result, as $t \to \infty$ each of the probabilities $W_k(t)$ converges to a non-zero value. Moreover, the set of equations (5.12) is practically restricted by a few sets (in our simulations, by $W_1(t)$ and $W_2(t)$ only, since the number of elements in $\mathcal{M}_2$ is already of the same order as the dimension of the total Hilbert space). For the case of a small number of subsets, in Ref. [1] the equations (5.12) have been modified and used to explicitly obtain an extremely detailed quench dynamics. In this case one can show that, on an intermediate time scale,

$$N_{pc}(t) \approx \exp(2\Gamma t), \tag{5.15}$$

which coincides with Eq. (5.14) for large $\mathcal{K}$ values. From the above analysis one can see that the key parameter in the quench dynamics is the parameter Γ. This parameter is closely related to the width of the LDoS. Indeed, the Local Density of States is defined by,

$$F_{k_0}(E) = \sum_{\alpha} |C_{k_0}^{\alpha}|^2 \delta(E - E^{\alpha}), \tag{5.16}$$

where $|k_0\rangle$ is an eigenstate of H_0. Thus, it is obtained by the projection of the initial state $|k_0\rangle$ onto the eigenstates of H. The concept of LDoS is extremely important in the analysis of the dynamical properties of many-body systems. The Fourier transform of the LDoS determines the survival probability of an initially excited many-body state, and it is effectively used in the study of fidelity in many applications. In particular, the inverse width $1/\Gamma$ of LDoS gives the characteristic time scale, which is associated with the depletion of the initial state, thus representing an early stage of thermalization [43]. Initially introduced

in atomic [54] and widely used in nuclear physics [55], it also serves as an important characteristic in other physical applications. As shown in many different papers (see for instance [56] and references therein), for systems with well defined classical limits, a classical analog of the LDoS can be defined and directly computed from the Hamilton equations of motion.

For isolated systems of interacting particles, described by a Hamiltonian $H = H_0 + V$, the form of LDoS changes on increasing the interaction strength V [19]. If for a weak, but not negligible, interaction the LDoS is typically a Lorentzian (apart from the tails which are due to the finite width of the energy spectrum), for a strong interaction (i.e. when the interaction energy becomes of the same order of the non-interacting one) its form becomes close to a Gaussian. Correspondingly, the width Γ of the LDoS can be estimated either using the Fermi golden rule, $\Gamma \approx 2\pi V^2 \rho_f$ where ρ_f is the density of the many-body states directly connected by V, or by the square root of the variance of LDoS, $\sigma = \sqrt{\sum H_{ij}^2}$ for $i \neq j$. When studying the TBRI model, this crossover was found to serve as the condition for the onset of strong quantum chaos, defined in terms of a pseudo-random structure of many-body eigenstates. For this reason, instead of Γ in our case one can use σ since the latter is much easier to estimate than the former. Thus, when comparing our data in Fig.5.12 with the predicted exponential dependence (5.15), we use the following expression:

$$\Gamma^2 = \sum_{k \neq j_0} H_{k,j_0}^2. \tag{5.17}$$

As will be shown below, the simple expression (5.15) nicely corresponds to numerical data demonstrating the exponential increase of N_{pc} in time.

Now let us discuss another important characteristic of the relaxation for finite systems, namely, the time scale over which the exponential growth of N_{pc} lasts. To do that, we have to estimate the saturation value $\overline{N_{pc}^{\infty}}$ of N_{pc} after the relaxation of the system to equilibrium.

This value, can be obtained by the time average performed after the saturation time t_s,

$$[\ \overline{N_{pc}^{\infty}}\ ]^{-1} = \lim_{T\to\infty} \frac{1}{T} \int_0^T dt\ [N_{pc}(t)]^{-1}. \tag{5.18}$$

An analytical expression, assuming non-degenerate energy levels, in terms of the eigenstates can be written as,

$$\overline{N_{pc}^{\infty}} = \left[2\sum_k (P_k^d)^2 - \sum_\alpha |C_{k_0}^\alpha|^4 \sum_k |C_k^\alpha|^4 \right]^{-1}. \tag{5.19}$$

This expression determines the total number of non-interacting many-body states inside the energy shell, excited in the process of equilibration.

Following [1], let us estimate the average value of N_{pc} after the relaxation, for the situation when the eigenstates are strongly chaotic. First of all let us notice that the second term in the r.h.s of Eq. (5.19) is roughly $1/\mathcal{D}$ times smaller than the first one, where $\mathcal{D}$ is the dimension of the many-body Hilbert space. This can be seen by taking uncorrelated components $C_k^\alpha \simeq (1/\sqrt{\mathcal{D}})e^{i\xi_{\alpha,k}}$, where $\xi_{\alpha,k}$ are random numbers. Thus, one gets,

$$2\sum_k (P_k^d)^2 = 2\sum_{\alpha,\beta,k} |C_{k_0}^\alpha|^2 |C_k^\alpha|^2 |C_{k_0}^\beta|^2 |C_k^\beta|^2 \simeq \frac{\mathcal{D}^3}{\mathcal{D}^4} \simeq \frac{1}{\mathcal{D}}, \tag{5.20}$$

while

$$\sum_{\alpha,k} |C_{k_0}^\alpha|^4 |C_k^\alpha|^4 \simeq \frac{\mathcal{D}^2}{\mathcal{D}^4} \simeq \frac{1}{\mathcal{D}^2} \tag{5.21}$$

As a result (taking the first of the above terms only), we arrive at the estimate,

$$\left[\ \overline{N_{pc}^{\infty}}\ \right]^{-1} \simeq 2\sum_k (P_k^d)^2. \tag{5.22}$$

Next, we assume a Gaussian shape for (i) the LDoS, (ii) the density of states for H_0 , and (iii) the density of states of H. These are realistic assumptions for chaotic many-body systems with random two-body interactions, such as the TBRI model close to the middle of the energy

spectrum. Obviously, in the tails of the spectrum the Gaussian approximation is not valid, see Fig.5.10. Since our interest is in the energy region far from the bottom of the spectrum, our assumptions are valid, at least when we interested in global characteristics of the dynamics, which in the first line depends on the width of the above shapes, and not on their details.

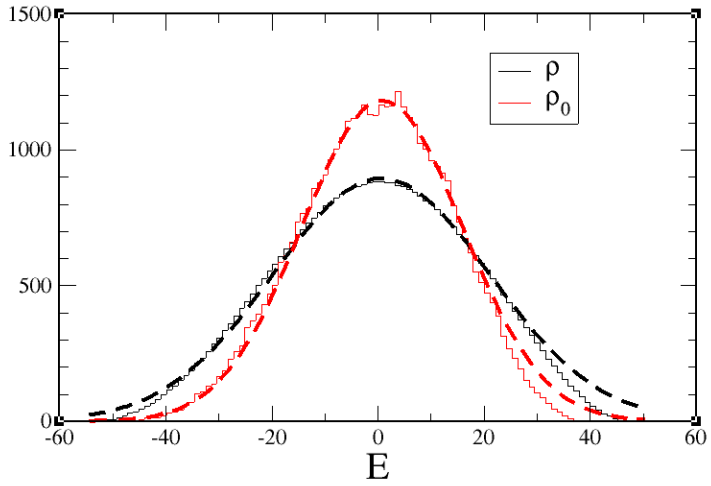

Figure 5.10: Histograms stands for interacting (black) and non-interacting (red) density of states for a system of $N = 8$ bosons in $M = 11$ single particle energy levels. Interaction strength is $v = 0.4$. The effective energy width of the Hamiltonians are : $\Delta_H = 98.78$ and $\Delta_{H_0} = 83.32$. Dashed lines are the Gaussian fit in the central region of the energy spectrum.

(i) For the LDoS we then assume

$$F_{k_0}(E) \simeq \frac{1}{\Gamma\sqrt{2\pi}} \exp\left\{-\frac{(E-\mathcal{E}_{k_0})^2}{2\Gamma^2}\right\}, \tag{5.23}$$

where Γ is the width of the LDoS and $\mathcal{E}_{k_0}$ is the energy of the non-interacting state. We also assume that Γ is independent of $\mathcal{E}_k$. Note that the LDoS is normalized, $\int F_k(E)dE = 1$.

(ii) The Gaussian shape for the non-interacting density of states $\rho_0(E)$ of width σ_0 is written as

$$\rho_0(E) = \frac{\mathcal{D}}{\sigma_0\sqrt{2\pi}} \exp\left\{-\frac{E^2}{2\sigma_0^2}\right\}. \tag{5.24}$$

(iii) The Gaussian density of states, characterized by a width σ, is such that

$$\rho(E) = \frac{\mathcal{D}}{\sigma\sqrt{2\pi}} \exp\left\{-\frac{E^2}{2\sigma^2}\right\}, \tag{5.25}$$

where for simplicity we set the middle of the spectrum at the energy $E = 0$. Both densities of states are normalized to the dimension of the Fock space,

$$\int \rho(E)dE = \int \rho_0(E_0)\ dE_0 = \mathcal{D}.$$

Numerical data confirm the Gaussian form of $\rho(E_0)$ and $\rho(E)$, for the TBRI model in the middle of the spectrum, see Fig. 5.10. As one can see, due to the interaction the energy spectrum increases its total width.

The above assumptions imply that in the continuum, one has

$$\begin{gathered}\textstyle\sum_\alpha |C^\alpha_{k_0}|^2 |C^\alpha_k|^2 \simeq \int dE\, \rho(E)^{-1} F_k(E) F_{k_0}(E) = \\ \frac{\sigma^2\Gamma^{-1}\mathcal{D}^{-1}}{\sqrt{2\sigma^2-\Gamma^2}} \exp\left\{-\frac{(\mathcal{E}_k)^2+(\mathcal{E}_{k_0})^2}{2\Gamma^2} + \frac{(\mathcal{E}_k+\mathcal{E}_{k_0})^2}{2\Gamma^2(2\sigma^2-\Gamma^2)}\right\} \equiv \mathcal{G}_{k_0}(\mathcal{E}_k)\end{gathered} \tag{5.26}$$

which is defined only for $2\sigma^2 > \Gamma^2$. We can then approximate

$$[\,\overline{N^\infty_{pc}}\,]^{-1} \simeq 2\sum_k (P^d_k)^2 \simeq 2\int dE\, \rho_0(E)\mathcal{G}^2_{k_0}(E). \tag{5.27}$$

Taking into account that $\sigma_0^2 = \sigma^2 - \Gamma^2$, Eq. (5.27) gives

$$\overline{N^\infty_{pc}} = C_1 \frac{\mathcal{D}\Gamma}{\sigma} e^{-\mathcal{E}^2_{k_0}/\Gamma^2} \tag{5.28}$$

with $C_1 = \sqrt{1/2 - \Gamma^2/4\sigma^2}$.

The time t_s, determining the onset of the saturation, can be estimated from the relation,

$$\exp(2\Gamma t_s) \approx \overline{N^\infty_{pc}}. \tag{5.29}$$

Considering the case for which $M \simeq 2N$, one gets an estimate for the maximal time [1]

$$t_s \approx \frac{N}{\Gamma}. \tag{5.30}$$

This is one of the important results, obtained in the frame of the discussed approach. As one can see, the characteristic time t_s is N times larger than the time $t_\Gamma \approx 1/\Gamma$ describing the early decrease of the return probability. The key point is that the time t_Γ has to be associated only with an initial process towards the true thermalization. In contrast, the latter emerges when the flow of probability fills *all* the subsets W_k that create the energy shell available in the thermalization process. This result can have important implications for addressing other issues such as the scrambling of information and the quantum butterfly effect.

5.5.3 Thermodynamic entropy versus diagonal entropy

Now let us discuss an important relation which has been discovered by analyzing the quench dynamics leading to thermalization. This relation links two entropies, S_{th} and S_{diag}. Here

$$S_{th} = \ln \overline{N_{pc}^{\infty}} \tag{5.31}$$

is the thermodynamic entropy characterizing the system *after* its relaxation to equilibrium and $\overline{N_{pc}^{\infty}}$ is the average number of basis states (eigenstates of H_0) in the stationary distribution. This number can be associated with the occupied 'volume" $\mathcal{V}_s(E)$ of the Hilbert space :

$$\mathcal{V}_s(E) \simeq \overline{N_{pc}^{\infty}}\delta_0, \tag{5.32}$$

where $\delta_0 = \Delta_{H_0}/\mathcal{D}$ is the non-interacting energy spacing, Δ_{H_0} is the effective width of the energy spectrum of H_0 and $\mathcal{D}$ is the dimension of the many-body Hilbert space.

As for the diagonal entropy S_{diag}, discussed in view of its relation to the Von Neumann entropy [57], it is given by,

$$S_{diag} = -\sum_{\alpha} |C_{k_0}^{\alpha}|^2 \ln |C_{k_0}^{\alpha}|^2. \tag{5.33}$$

Note that the diagonal entropy is the Shannon entropy of the set of probabilities $w_{k_0}(E^{\alpha}) = |C_{k_0}^{\alpha}|^2$ obtained by the projection of the non-interacting state $|k_0\rangle$ of H_0 onto the eigenstates of H. With the Shannon entropy we can built the entropic localization length

$$\ell_H = \exp\left(S_{diag}\right), \tag{5.34}$$

giving the number of eigenstates of H excited by the initial basis state [53]. Thus, the volume occupied by the initial state is $\mathcal{V}_i(E) \simeq \ell_H \delta$, where δ is the energy spacing estimated as $\delta \simeq \Delta_H/\mathcal{D}$. Since the two volumes are equal, $\overline{N_{pc}^{\infty}}\Delta_{H_0} = \ell_H \Delta_H$, we arrive at the following relation:

$$S_{th} = S_{diag} + \ln(\Delta_H/\Delta_{H_0}), \tag{5.35}$$

where Δ_H and Δ_{H_0} are the widths of the energy spectra of H and H_0, respectively. A similar correction due to the difference between Δ_H and Δ_{H_0} also appeared in other context [58].

Our numerical study of the quench dynamics of the t-LL model demonstrates that $N_{pc}(t)$ oscillates in time in the MF regime ($n/g \gg 1$) as shown in Fig.5.11. In contrast, it grows exponentially fast in the TG regime ($n/g \lesssim 1$, see Fig. 5.12), after a short time where, due to the standard perturbation theory, the time-dependence is quadratic in time. This exponential growth lasts up to some time t_s after which a clear saturation of N_{pc} emerges, together with irregular fluctuations around its mean value. In order to reduce these fluctuations which are due to different initial conditions (various values of j_0), we have performed the average $\langle N_{pc} \rangle$ over all those initial non-interacting basis states with the same energy.

First, the numerical data clearly manifest a very good correspondence to the analytical estimates of the exponential increase of $N_{pc}(t)$ occurring for $t \ll t_s$. Second, the relaxation time t_s roughly corresponds to the estimate $t_s \approx N/\Gamma$ (specifically, to $\Gamma t_s \approx N$ with $N = 9$). Finally, the relation (5.35) between the diagonal and thermodynamic entropies holds with a very good accuracy. All these results are highly non-trivial since they are obtained for the t-LL model which is non-random. Specifically, one can show that the non-diagonal matrix elements of the total Hamiltonian are strongly correlated. For the case shown in Fig.5.12 diagonal and off-diagonal Hamiltonian matrix elements take the values from a set with very few elements, as one can see from the plots shown in Fig.5.4. It is important to note that the validity of our analytical expression holds also in this case where the non-interacting density of states is a set of $\delta-$functions (and certainly not a Gaussian)

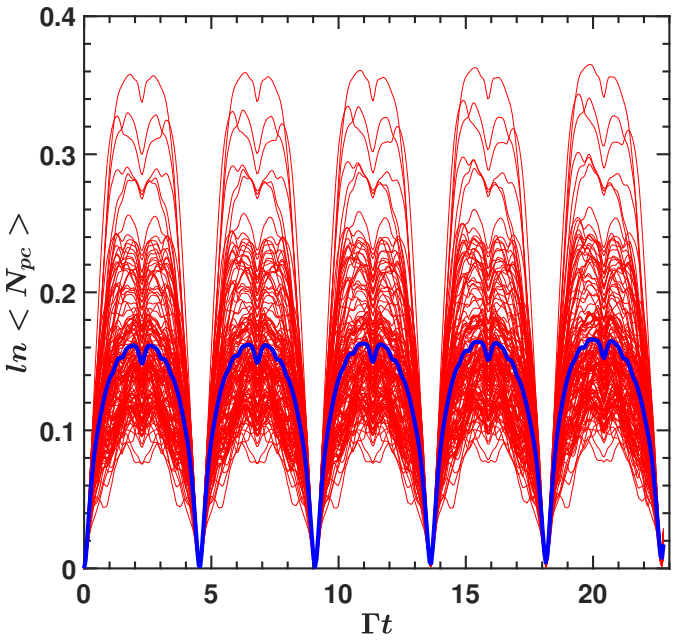

Figure 5.11: Time dependence of $\ln\langle N_{pc}\rangle$ for the t-LL model for weak interaction (MF regime). On x-axis we put the dimensionless time Γt where Γ is the width of the LDoS averaged over the degenerate initial states. The average (blue curve) has been done over all initial degenerate states having the same energy E_0 close to the band center (with $j_0 \approx 4050$). Here we considered $N = 9$ particles in $\ell = 13$ momentum levels, $n/g = 10$, for a fixed total momentum $P = 1$ (the matrix size is 8122). The normalized diagonal entropy $S_{diag} + \ln(\Delta_H/\Delta_{H_0}) = 2.75 \pm 1$ does not correspond to the equilibrium value since for this interaction strength the eigenstates involved in the dynamics are not chaotic.

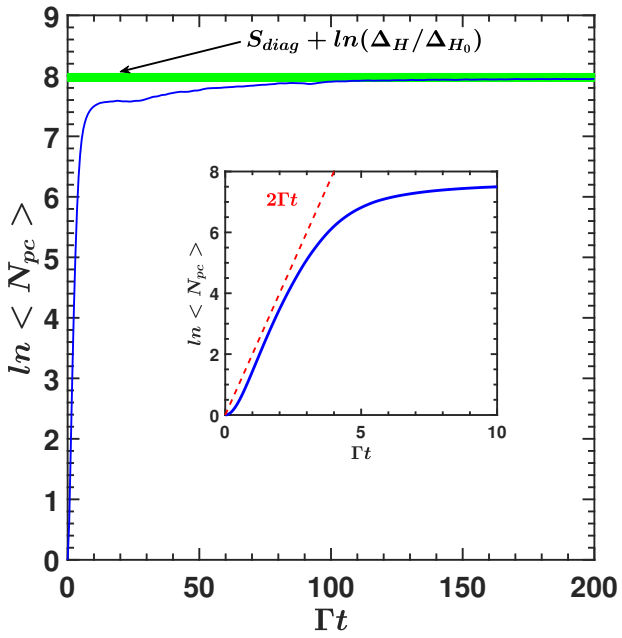

Figure 5.12: Time dependence of $\ln\langle N_{pc}\rangle$ for the t-LL model. On x-axis we put the dimensionless time Γt where Γ is the width of the LDoS averaged over the degenerate initial states. The average has been done over all initial degenerate states having the same energy E_0 close to the band center (with $j_0 \approx 4050$). Inset: the early stage of the evolution of $\ln\langle N_{pc}\rangle$, in comparison with linear dependence $2\Gamma t$ (red dashed line). Here we considered $N = 9$ particles in $\ell = 13$ momentum levels, $n/g = 0.5$, for a fixed total momentum $P = 1$ (the matrix size is 8122). Horizontal green thick line represents the normalized diagonal entropy $S_{diag} + \ln(\Delta_H/\Delta_{H_0})$, the thickness corresponds to one standard deviation due to different initial states. In computing Δ_H and Δ_{H_0} we excluded a number of energies close to the band edges.

5.6 Occupation Number

As shown above the interaction act as a thermal bath leading to thermalization. In the following we will see that we can then define an effective energy, dependent on the inter-particle interaction, via the Bose-Einstein distribution.

Our conserved quantity are the total number of particles, the total momentum and total energy:

$$\begin{cases} \sum_s n_s = N \\ \sum_s s n_s = P \\ \sum_s \epsilon_s n_s = E \end{cases} \tag{5.36}$$

Due to the conservation of total momentum, the generalized Bose-Einstein distribution will be:

$$p_s = \frac{g_s}{\exp(\alpha - \gamma s + \beta \epsilon_s) - 1} \quad , \quad g_s = 1 \tag{5.37}$$

5.6.1 Eigenstates

To solve the system of Eq. 5.36, in our case the total number of particle is fixed $N = 9$, the total momentum $P = 1$, and the dressed energy is calculated for the single eigenstate (since we will make an average between multiple eigenstates with close energies, we will consider the average of the energies) as

$$\begin{aligned} \tilde{E}_\alpha &= \sum_s \epsilon_s n_s^{(\alpha)} = \sum_s \sum_k \epsilon_s |C_k^\alpha|^2 n_s^{(k)} \\ &= \sum_k |C_k^\alpha|^2 \sum_s \epsilon_s n_s^{(k)} = \sum_k |C_k^\alpha|^2 E_k \end{aligned} \tag{5.38}$$

Then we compare the results (p_s) with the occupation number:

$$n_s^{(\alpha)} = \sum_k |C_k^\alpha|^2 n_s^{(k)} \quad , \quad \sum_s \epsilon_s n_s^{(k)} \equiv E_k \tag{5.39}$$

Numerical computations show that in the middle of the spectrum we have a very good correspondence of the exact eigenstates with the generalized Bose-Einstein distribution with fixed number of particle N, momentum P and energy $E = \tilde{E}_\alpha$ "dressed" energy defined in Eq. 5.38.

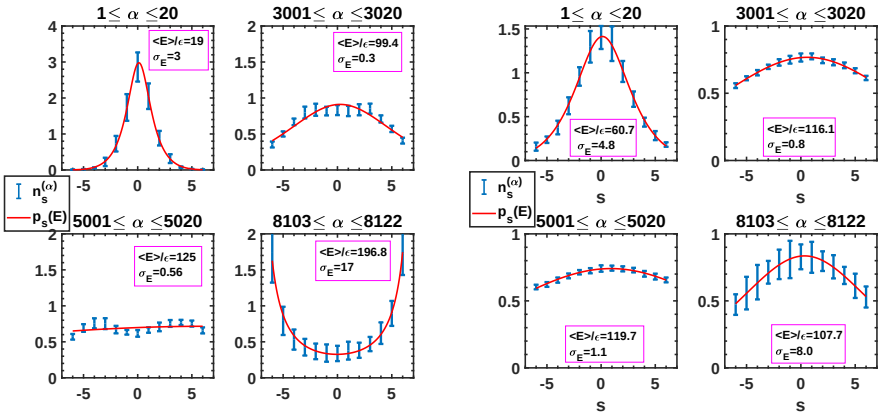

Figure 5.13: Blue error bar: mean distribution (with relative error bars) of the eigenstates shown in the upper part of the figures compared with the Red line: distribution obtained through the numerical solution of the system of Eq.5.36 with mean Energy $E =< \tilde{E}_\alpha >$ over the chosen states. In the insets it's shown the mean Dressed Energy and the relative error σ_E. $N = 9$ particles in $\ell = 13$ single particle states, with total momentum $P = 1$ and medium interaction $n/g = 0.5$ (left), strong interaction $n/g = 0.05$ (right)

5.6.2 Time Evolution

Since previous results show thermalization for some interaction, we expect a thermalization also in the occupation number distribution. We calculate the "time dependent dressed" energy and the evolved occupation number distribution through the projection in the unperturbed many-body basis:

$$\tilde{E}(t) = \sum_k |c_k(t)|^2 E_k \quad , \quad n_s(t) = \sum_k |c_k(t)|^2 n_s^k \tag{5.40}$$

where:

$$c_k(t) =< k|\psi(t) >=< k|e^{-iHt}|k_{in} > \tag{5.41}$$

We can then calculate the time evolved unperturbed Energies distribution defined as (notice that the "time dependent dressed" energy defined above is the mean value of this distribution):

$$P(E_k, t) = \sum_k |c_k(t)|^2 \delta(E - E_k) \tag{5.42}$$

while the unperturbed Energies distribution is:

$$P_0(E_k) = \frac{1}{N_{states}} \sum_k \delta(E - E_k) \tag{5.43}$$

a)

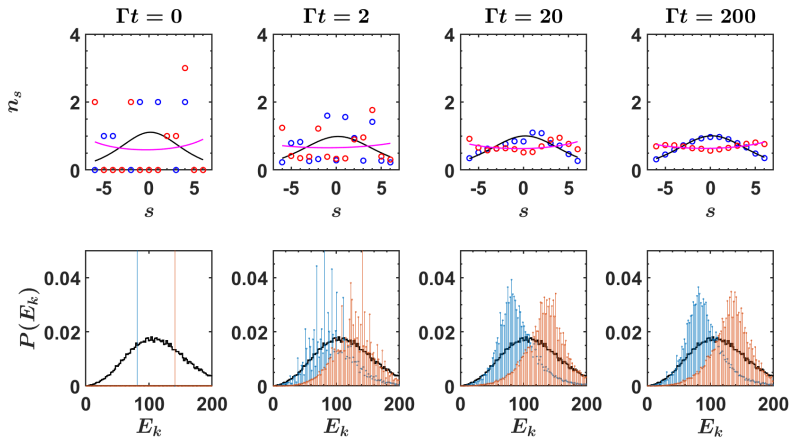

b)

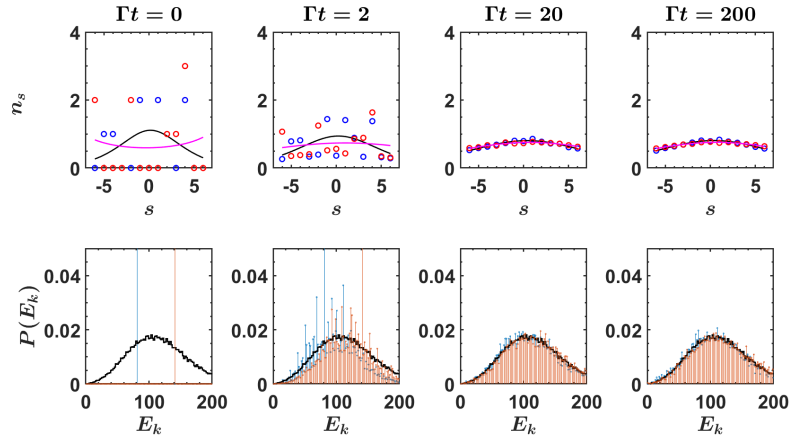

Figure 5.14: Upper panels) Blue and Red dots: occupation distribution for two different initial states, compared with Black and Purple curves: distribution obtained through the numerical solution of the system of Eq.5.36 with Energy $E = \tilde{E}(t)$ from Eq.5.40 of the time evolved initial state.
Lower panels) Blue and Red bins: Projection of the time evolved state into the non interacting many body basis (Eq.5.42). Black stair: Many body non interactive Energies distribution (Eq.5.43).
$N = 9$ particles in $\ell = 13$ single particle states, with total momentum $P = 1$ and interactions $n/g = 0.5$ (a) and $n/g = 0.05$ (b) .

Chapter 6

Summary

We started introducing some interesting results obtained in the study of the Bethe Ansatz to have a better understanding of the model. Studying the spectrum we found important symmetries which make the calculation of the spectrum easier. We then address the problem of genericity of Poisson distribution for level spacing distribution of integrable systems. In particular, we show that for Lieb Liniger model, Poisson distribution occurs only for particular interaction strengths and particular energy range.

We have studied the truncated Lieb Liniger model (t-LL) with a finite number of particles in a finite number of momentum states which is originated from the completely integrable Lieb-Liniger model. By studying the quench dynamics in the region where the many-body eigenstates can be considered as strongly chaotic, we have found that the time evolution is quite similar to that recently found for the random TBRI, as well as for the deterministic XXZ model of interacting 1D spins-1/2 [20, 21]. Specifically, the number of components in the wave packets evolving in the Hilbert space, increases exponentially in time with a rate given by twice the width of the LDoS related to the initial state of the non-interacting many-body Hamiltonian H_0. This growth lasts approximately until the saturation time t_s which is much larger than the inverse width of the LDoS characterizing the initial decay of the survival probability. Both the rate of the exponential

increase and the characteristic time t_s for the onset of equilibration, nicely correspond to our semi-analytically estimates.

By studying the process of relaxation of the system to the equilibrium, we have discovered a remarkable relation between the thermodynamic entropy S_{th} (defined in terms of the number of principal components N_{pc} in the wave function) of the system *after the equilibration*, and the diagonal entropy S_{diag} related to an *initial many-body state*. This relation (5.35) establishes a direct link between statistical and thermodynamical properties, and seems to be generic, valid for both deterministic and random many-body systems. Recently, another relation between the diagonal entropy and the GGE entropy was found in a fully integrable 1D Ising model in a transverse magnetic field [61, 62]. Thus, a further study of the relevance of the diagonal entropy to the thermodynamic properties of many-body systems seems to be very important, especially, in view of possible experimental studies of the onset of thermalization in isolated systems.

We have shown that the generalized Bose-Einstein distribution, known to appear in the thermodynamic limit, emerges on the level of an individual eigenstate in the truncated Lieb-Liniger model. This happens when the inter-particle interaction is strong enough to lead to the onset of chaotic many-body eigenstates in the basis defined by the chosen single-particle spectrum. For the eigenstates we computed the correspondent occupation number distribution and verified that they can be successfully described by a generalized Bose-Einstein distribution with a suitable "dressed" energy dependent on the inter-particle interaction. We also have shown that after the thermalization time, the evolved state, due to the interaction, reach a thermal state.

Bibliography

[1] F. Borgonovi, F.M. Izrailev, and L.F. Santos, Exponentially fast dynamics in the Fock space of chaotic many-body systems, Phys. Rev. E **99**, 010101(R) (2019).

[2] M. Horoi, V. Zelevinsky, and B.A. Brown, Chaos vs thermalization in the nuclear shell model, Phys. Rev. Lett. **74**, 5194 (1995).

[3] V. Zelevinsky, B.A. Brown, N. Frazier, and M.Horoi, The nuclear shell model as a testing ground for many-body quantum chaos, Phys. Rep. **276**, 85 (1996).

[4] V.V. Flambaum and F.M. Izrailev, Statistical theory of finite Fermi systems based on the structure of chaotic eigenstates, Phys. Rev. E **56**, 5144 (1997).

[5] V. Zelevinsky, Quantum chaos and complexity in nuclei, Annu. Rev. Nucl. **46**, 237 (1996).

[6] F. Borgonovi, I. Guarneri, F.M. Izrailev, and G. Casati, Chaos and thermalization in a dynamical model of two interacting particles, Phys. Lett. A **247**, 140 (1998).

[7] G.F. Gribakin, A.A. Gribakina, and V.V. Flambaum, Quantum chaos in multicharged ions and statistical approach to the calculation of electron-ion resonant radiative recombination, Aust. J. Phys. **52**, 443 (1999).

[8] M. Rigol, V. Dunjko, and M. Olshanii, Thermalization and its mechanism for generic isolated quantum systems, Nature **452**, 854 (2008).

[9] A. Polkovnikov, K. Sengupta, A. Silva, and M. Vengalattore, Colloquium: Nonequilibrium dynamics of closed interacting quantum systems, Rev. Mod. Phys. **83**, 863 (2011).

[10] L. D'Alessio, Y. Kafri, A. Polkovnikov, and M. Rigol, From quantum chaos and eigenstate thermalization to statistical mechanics and thermodynamics, Advances in Physics, **65**, 239 (2016).

[11] D.J.Luitz and Y.B.Lev, Anomalous Thermalization in Ergodic Systems, Phys. Rev. Lett. **117**, 170404 (2016).

[12] D.A. Abanin, E. Altman, I. Bloch, and M. Serbyn, Colloquium: Many-body localization, thermalization, and entanglement, Rev. Mod. Phys. **91**, 021001 (2019).

[13] M. Greiner, O. Mandel, T.W. Hansch, and I. Bloch, Collapse and revival of the matter wave field of a Bose - Einstein condensate, Nature **419**, 51 (2002).

[14] S. Trotzky *et. al.*, Probing the relaxation towards equilibrium in an isolated strongly correlated one-dimensional Bose gas, Nature Phys. **8**, 325 (2012).

[15] M. Gring, *et al.*, Relaxation and Prethermalization in an Isolated Quantum System, Science **337**, (2012) 1318.

[16] A.M. Kaufman *et al.*, Quantum thermalization through entanglement in an isolated many-body system, Science, **353**, 794 (2016).

[17] R. Nandkishore and D.A. Huse, Many-Body Localization and Thermalization in Quantum Statistical Mechanics, Annual Review of Condensed Matter Physics **6**, 15 (2015).

[18] T. Kinoshita, T. Wenger and D. S. Weiss, A quantum Newton's cradle. Nature **440**, 900â€“903 (2006).

[19] F. Borgonovi, F. M. Izrailev, L. F. Santos, and V. G. Zelevinsky, Quantum chaos and thermalization in isolated systems of interacting particles, Phys. Rep. **626**, 1 (2016).

[20] L. F. Santos, F. Borgonovi, and F. M. Izrailev, Onset of chaos and relaxation in isolated systems of interacting spins: Energy shell approach, Phys. Rev. E **85**, 036209 (2012).

[21] L. F. Santos, F. Borgonovi, and F. M. Izrailev, Chaos and statistical relaxation in quantum systems of interacting particles, Phys. Rev. Lett. **108**, 094102 (2012).

[22] E.P. Wigner, Characteristic vectors of bordered matrices with infinite dimensions, Ann. of Math. **62**, 548 (1955); Characteristics vectors of bordered matrices with infinite dimensions II, Ann. of Math. **65**, 203 (1957); On the distribution of the roots of certain symmetric matrices, Ann. of Math. **67**, 325 (1958).

[23] F.J. Dyson, Statistical theory of the energy levels of complex systems I, J. Math. Phys. **3**, 140 (1962); Statistical theory of the energy levels of complex systems II, J. Math. Phys. **3**, 157 (1962); Statistical theory of the energy levels of complex systems III, J. Math. Phys. **3**, 166 (1962).

[24] J. B. French and S. S. M. Wong, Validity of random matrix theories for many-particle systems, Phys. Lett. B bf 33, 449 (1970).

[25] O. Bohigas and J. Flores, Spacing and individual eigenvalue distributions of two-body random Hamiltonians, ibid. **35**, 383 (1971); Two-body random Hamiltonian and level density, **34**, 261 (1971).

[26] T. A. Brody, J. Flores, J. B. French, P. A. Mello, A. Pandey, and S. S. M. Wong, Random-matrix physics: Spectrum and strength fluctuations, Rev. Mod. Phys. **53**, 385 (1981).

[27] L. Benet and H. A. Weidenmueller, Review of the k-body embedded ensembles of Gaussian random matrices, J. Phys. A: Math. Gen. **36**, 3569 (2003).

[28] N. D. Chavda, V. K. B. Kota, and V. Potbhare, Thermalization in one- plus two-body ensembles for dense interacting boson systems, Phys. Lett. A **376**, 2972 (2012).

[29] V. K. B. Kota and N. D. Chavda, Embedded random matrix ensembles from nuclear structure and their recent applications, Int. J. Mod. Phys. E **27**, 1830001 (2018).

[30] M. Vyas, and V. K. B. Kota, Quenched many-body quantum dynamics with k-body interactions using q-Hermite polynomials, J. Stat. Mech. **2019**, 103103.

[31] V. K. B. Kota, *Embedded Random Matrix Ensembles in Quantum Physics* (Springer-Verlag, Heidelberg 2014).

[32] S. Sachdev and J. Ye, Gapless spin-fluid ground state in a random quantum Heisenberg magnet, Phys. Rev. Lett. **70**, 3339 (1993).

[33] A. Kitaev, A simple model of quantum holography, KITP Entangled15, http://online.kitp.ucsb.edu/entangled15.

[34] Y. Jia and J.J.M. Verbaarschort, Spectral Fluctuations in the Sachdev-Ye-Kitaev Model, arXiv:1912.11923 [hep-th] (2019).

[35] S. H. Shenker and D. Stanford, Black holes and the butterfly effect, JHEP **03**, 067 (2014).

[36] J. Cotler, N. Hunter-Jones, J. Liu, and B. Yoshida,Chaos, Complexity, and Random Matrices, JHEP **11**, 048 (2017).

[37] M. Blake, R. A. Davison, S. Grozdanov, and H. Liu, Many-body chaos and energy dynamics in holography, JHEP **10**, 035 (2018).

[38] A. Larkin and Yu. N. Ovchinnikov, Quasiclassical Method in the Theory of Super- conductivity, Eksp. Teor. Fiz. **55**, 2262 (1969) [Sov. Phys. JETP 28, 1200 (1969)].

[39] J. Maldacena, S. H. Shenker, and D. Stanford, A bound on chaos, J. High Energy Phys. 2016, **106** (2016).

[40] E.B. Rozenbaum, S. Ganeshan, and V. Galitski, Lyapunov exponent and out-of-time-ordered correlator's growth rate in a chaotic system, Phys. Rev. Lett. **118**, 086801 (2017).

[41] B. Swingle, Unscrambling the physics of out-of-time- order correlators, Nat. Phys. **14**, 988 (2018).

[42] D. Rossini, S. Suzuki, G. Mussardo, G.E. Santoro and A. Silva, Long time dynamics following a quench in an integrable quantum spin chain: Local versus nonlocal operators and effective thermal behavior, Phys. Rev. B **82**, 144302 (2010)

[43] F. Borgonovi, F.M. Izrailev, and L.F. Santos, Timescales in the quench dynamics of many-body quantum systems: Participation ratio versus out-of-time ordered correlator, Phys. Rev. E **99**, 052143 (2019).

[44] E. H. Lieb and W. Liniger, Exact Analysis of an Interacting Bose Gas. I. The General Solution and the Ground State, Phys. Rev. **130**, 1605 (1963).

[45] E. H. Lieb, Exact Analysis of an Interacting Bose Gas. II. The Excitation Spectrum, **130**, 1616 (1963).

[46] M. Girardeau, Relationship between Systems of Impenetrable Bosons and Fermions in One Dimension, J. Math. Phys. **1**, 516 (1960).

[47] H. A. Bethe, Zur Theorie der Metalle, Z. Phys **71**, 205 (1931).

[48] V. E. Korepin, N. M. Bogoliubov, and A. G. Izergin, Quantum Inverse Scattering Method and Correlation Functions (Cambridge University Press, Cambridge, UK, 1993).

[49] A. Gorlitz et al., Realization of Bose-Einstein Condensates in Lower Dimensions, Phys. Rev. Lett. **87**, 130402 (2001).

[50] T. Kinoshita, T. Wenger, and D.S. Weiss, Observation of a one-dimensional Tonks-Girardeau gas, Science **305**, 1125 (2004),

[51] B. Paredes et al., Tonks-Girardeau gas of ultracold atoms in an optical lattice, Nature (London) **429**, 377 (2004).

[52] N.J. Robinson, A.J.J.M. de Klerk, and J.-S. Caux, On computing non-equilibrium dynamics following a quench, arXiv:1911.11101 (2019).

[53] V.V.Flambaum and F.M.Izrailev, Entropy production and wave packet dynamics in the Fock space of closed chaotic many-body systems, Phys. Rev. E, **64** (2001) 036220.

[54] O.K. Rice, Predissociation and the crossing of molecular potential energy curves, J. Chem. Phys. **1** (1933) 375.

[55] A. Bohr and B.R. Mottelson, *Nuclear Structure*, Benjamin, New York, 1969.

[56] F.M.Izrailev, Quantum-Classical Correspondence for Isolated Systems of Interacting Particles: Localization and Ergodicity in Energy Space, Proceedings of the Nobel Simposia "Quantum Chaos Y2K", Physica Scripta, T **90**, 95 (2001).

[57] A. Polkovnikov, Microscopic diagonal entropy and its connection to basic thermodynamic relations, Annals of Physics **326**, 486 (2011).

[58] F.Borgonovi and F.M.Izrailev, Classical statistical mechanics of a few-body interacting spin model, Phys. Rev. E **62**, 6475 (2000).

[59] V.V. Flambaum, G.F. Gribakin, and F.M. Izrailev, Correlations within Eigenvectors and Transition Amplitudes in the Two-Body Random Interaction Model, Phys. Rev. **E 53**, 5729 (1996).

[60] G.P. Berman, F. Borgonovi, F.M. Izrailev, and A. Smerzi, Irregular Dynamics in a One-Dimensional Bose System, Phys. Rev. Lett. **92**, (2004) 030404.

[61] M. Kormos, L. Bucciantini, and P. Calabrese, Stationary entropies after a quench from excited states in the Ising chain, EPL **107**, 40002 (2014).

[62] L. Piroli, E. Vernier, P. Calabrese, and M. Rigol, Correlations and diagonal entropy after quantum quenches in XXZ chains, Phys. Rev. B **95**, 054308 (2017).

[63] E. H. Lieb and W. Liniger, Phys. Rev. **130**, 1605 (1963); E. H. Lieb, ibid. **130**, 1616 (1963).

[64] F. Schreck et al., Phys. Rev. Lett. **87**, 080403 (2001); A. Gorlitz et al., Phys. Rev. Lett. **87**, 130402 (2001); M. Greiner et al., Phys. Rev. Lett. **87**, 160405 (2001); H. Moritz et al., Phys. Rev. Lett. **91**, 250402 (2003); B.L. Tolra et al., Phys. Rev. Lett. **92**, 190401 (2004); T. Stoferle et al., Phys. Rev. Lett. **92**, 130403 (2004), T. Kinoshita, T. Wenger, and D.S. Weiss, Science **305**, 1125 (2004), B. Paredes et al., Nature (London) **429**, 377 (2004).

[65] M. Olshanii, Phys. Rev. Lett. **81**, 938 (1998); D.S. Petrov, G.V. Schlyapnikov, and J.T.M. Valraven, Phys. Rev. Lett. **85** 3745 (2000), V. Dunjko, V. Lorent, and M. Olshanii, Phys. Rev. Lett. **86** 5413 (2001).

[66] T. Kinoshita, T. Wenger, and D.S. Weiss, Nature (London) **440**, 900 (2006).

[67] G. P. Berman, F. Borgonovi, F. M. Izrailev and A. Smerzi, Phys. Rev. Lett. **92**, 030404 (2004).

[68] G. Casati, F. Valz-Gris, I. Guarneri, Lett. Nuovo Cimento **28**, 279 (1980).

[69] O. Bohigas, M. J. Giannoni, C. Schmit, Characterization of chaotic quantum spectra and universality of level fluctuation laws, Phys. Rev. Lett. **52**, 1 (1984).

[70] F. Borgonovi, F. M. Izrailev and L. F. Santos, Phys. Rev. E **99**, 010101(R) (2019).

[71] F. Borgonovi and F. M. Izrailev, Phys. Rev. E **99**, 012115 (2019).

[72] V. Zelevinsky, B. A. Brown, N. Frazier, M. Horoi, The nuclear shell model as a testing ground for many-body quantum chaos, Phys. Rep. 276 (1996) 85-176.

[73] M. C. Gutzwiller, Chaos in Classical and Quantum Mechanics, Springer-Verlag, New York, 1990.

[74] F. Haake, Quantum Signatures of Chaos, Springer-Verlag, Berlin, 1991.

[75] H. J. Stöckmann, Quantum Chaos: An Introduction, Cambridge University Press, Cambridge, 2006.

[76] L. E. Reichl, The transition to chaos: conservative classical systems and quantum manifestations, Springer, New York, 2004.

[77] H. J. Metcalf, P. van der Straten, Laser Cooling and Trapping, Springer-Verlag, New York, 1999.

[78] E. P. Wigner, On a class of analytic functions from the quantum theory of collisions, Ann. Math. **53** (1) (1951) 36-67.

[79] E. P. Wigner, Characteristic vectors of bordered matrices with infinite dimensions, Ann. Math. **62** (3) (1955) 548-564.

[80] E. P. Wigner, Characteristics vectors of bordered matrices with infinite dimensions II, Ann. Math. **65** (2) (1957) 203-207.

[81] E. P. Wigner, On the distribution of the roots of certain symmetric matrices, Ann. Math. **67** (2) (1958) 325-327.

[82] A. M. Lane, R. G. Thomas, E. P. Wigner, Giant resonance interpretation of the nucleon-nucleus interaction, Phys. Rev. **6798** (1955) 693-701.

[83] Y. V. Fyodorov, O. A. Chubykalo, F. M. Izrailev, G. Casati, Wigner random banded matrices with sparse structure: Local spectral density of states, Phys. Rev. Lett. **6776** (1996) 1603-1606.

[84] C. E. Porter, Statistical Theories of Spectra: Fluctuations, Academy Press, New York, 1965.

[85] M. L. Mehta, Random Matrices, Academic Press, Boston, 1991.

[86] J. French, S.Wong, Some random-matrix level and spacing distributions for fixed-particle-rank interactions, Phys. Lett. B **35** (1) (1971) 5-7.

[87] K. Mon, J. French, Statistical properties of many-particle spectra, Ann. Phys. (N.Y.) **95** (1) (1975) 90 - 111.

[88] V. V. Flambaum, A. A. Gribakina, G. F. Gribakin, M. G. Kozlov, Structure of compound states in the chaotic spectrum of the ce atom: Localization properties, matrix elements, and enhancement of weak perturbations, Phys. Rev. A **50** (1994) 267-296.

[89] C. W. Johnson, G. F. Bertsch, D. J. Dean, Orderly spectra from random interactions, Phys. Rev. Lett.**80** (1998) 2749-2753.

[90] V. Zelevinsky, A. Volya, Nuclear structure, random interactions and mesoscopic physics, Phys. Rep. **391** (2004) 311 - 352.

[91] J. Oitmaa, O. P. Sushkov, Two-dimensional randomly frustrated spin- 1/2 Heisenberg model, Phys. Rev. Lett. **87** (2001) 167206.

[92] M. Horoi, V. Zelevinsky, Random interactions explore the nuclear landscape: Predominance of prolate nuclear deformations, Phys. Rev. C **81** (2010) 034306.

[93] V. Abramkina, A. Volya, Quadrupole collectivity in the two-body random ensemble, Phys. Rev. C **84** (2011) 024322.

[94] R. Bijker, A. Frank, Mean-field analysis of interacting boson models with random interactions, Phys. Rev. C **64** (2001) 061303.

[95] G. Casati, B. V.Chirikov, F. M.Izrailev, J. Ford, Stochastic Behavior of a Quantum Pendulum under a Periodic Perturbation, Lect. Notes in Phys. vol **93**, 334-352, Springer, Heidelberg, 1979.

[96] B. V. Chirikov, F. M. Izrailev, D. L.Shepelyansky, Dynamical stochasticity in classical and quantum mechanics, Sov. Scient. Rev. C **2** (4) (1981) 209-267.

[97] F. M. Izrailev, Simple models of quantum chaos: Spectrum and eigenfunctions, Phys. Rep. **196** (1990) 299-392.

[98] S. W. McDonald, A. N. Kaufman, Spectrum and eigenfunctions for a Hamiltonian with stochastic trajectories, Phys. Rev. Lett. **42** (1979) 1189-1191.

[99] G. Casati, F. Valz-Gris, I. Guarneri, On the connection between quantization of nonintegrable systems and statistical theory of spectra, Lett. Nuovo Cim. **28** (1980) **279**.

[100] M. V. Berry, M. Tabor, Level clustering in the regular spectrum, Proc. R. Soc. London Ser. A **356** (1977) 375.

[101] G. Casati, B. V. Chirikov, I. Guarneri, Energy-level statistics of integrable quantum systems, Phys. Rev. Lett. **54** (1985) 1350-1353.

[102] M. V. Berry, Regular and irregular semiclassical wavefunctions, J. Phys. A **10** (1977) 2083.

[103] F. Borgonovi, G. Casati, B. Li, Diffusion and localization in chaotic billiards, Phys. Rev. Lett. **6777** (1996) 4744.

[104] M. Shapiro, G. Goelman, Onset of chaos in an isolated energy eigenstate, Phys. Rev. Lett. **53** (1984) 1714-1717.

[105] B. V. Chirikov, An example of chaotic eigenstates in a complex atom, Phys. Lett. A **108** (2) (1985) 68 - 70.

[106] A. Bohr, B. R. Mottelsoni, Nuclear Structure, Benjamin, New York, 1969.

[107] V. V. Flambaum, F. M. Izrailev, G. Casati, Towards a statistical theory of finite Fermi systems and compound states: Random two-body interaction approach, Phys. Rev. E **54** (1996) 2136-2139.

[108] V. V. Flambaum, F. M. Izrailev, Distribution of occupation numbers in finite Fermi systems and role of interaction in chaos and thermalization, Phys. Rev. E **55** (1997) R13-R16.

[109] V. V. Flambaum, F. M. Izrailev, Statistical theory of finite Fermi systems based on the structure of chaotic eigenstates, Phys. Rev. E **56** (1997) 5144.

[110] N. N. Bogolubov, On Some Statistical Methods in Mathematical Physics, Ukr. SSR Academy of Sciences, Kiev (in Russian), 1945.

[111] N. N. Bogolubov, On some problems related to the foundation of statistical mechanics, in: Proceedings of the Second International Conference on Selected Problems of Statistical Mechanics, JINR, Dubna, 1981.

[112] M. Aizenman, S. Goldstein, J. L. Lebowitz, Ergodic properties of an infinite one dimensional hard rod system, Commun. Math. Phys. **39** (4) (1975) 289-301.

[113] S. Goldstein, Space-time ergodic properties of systems of infinitely many independent particles, Commun. Math. Phys. **39** (4) (1975) 303-327.

[114] B. V. Chirikov, Transient chaos in quantum and classical mechanics, Found. of Phys. **16** (1986) 39.

[115] N. N. Bogolubov, Selected papers, Naukova Dumka, Kiev **2** (1970) 77.

[116] B. V. Chirikov, Linear and nonlinear dynamical chaos, Open. Sys. & Information Dyn. **4** (1997) 241-280.

[117] M. Srednicki, Chaos and quantum thermalization, Phys. Rev. E **50** (1994) 888.

[118] F. M. Izrailev, Quantum-classical correspondence for isolated systems of interacting particles: Localization and ergodicity in energy space, Phys. Scr. T**90** (2001) 95-104.

[119] L. Corps, A. Relaño, Distribution of the ratio of consecutive level spacings for different symmetries and degrees of chaos, Phys. Rev. E **101** (2020) 2470-0053

[120] T. H. Seligman, J. J. M. Verbaarschot and M. R. Zirnbauer, Spectral fluctuation properties of Hamiltonian systems: the transition region between order and chaos, J. Phys. A (1985)

Oficio No. IF-SACAD137/2021

Asunto: **Oficio de modalidad de titulación.**

MTRA. MARÍA ELENA RUÍZ VELASCO
Directora de Administración Escolar
Benemérita Universidad Autónoma de Puebla
Presente

El que suscribe, Director del Instituto de Física "Ing. Luis Rivera Terrazas", le informo que el **M.C. SAMY MAILOUD SEKKOURI**, matrícula: **217570145**, presentará y defenderá su examen de grado de **DOCTORADO EN CIENCIAS (FÍSICA)** en la **MODALIDAD DE PRESENTACIÓN DE TESIS**, cuyo título es: ***"Dynamical Aspects of Thermalization in Isolated Systems of Interacting Bose Particles"***, que se llevará a cabo el día **lunes 28 de junio de 2021 a las 09:00 horas**. Hago de su conocimiento que dicho **EXAMEN DE GRADO SERÁ EN LÍNEA** a través de la plataforma *Google Meet*, debido a la emergencia sanitaria por el virus SARS CoV-2. El Jurado Examinador estará integrado por:

Dra. Lea Ferreira dos Santos	**Presidenta**
Dr. José Luis Eustolio Carrillo Estrada	**Secretario**
Dr. José Antonio Méndez Bermúdez	**Vocal**
Dr. Felipe Pacheco Vázquez	**Vocal**
Dr. Félix Izrailev	**Vocal**

Sin otro asunto que el particular, aprovecho la ocasión para enviarle un cordial saludo.

A T E N T A M E N T E
"Pensar Bien, Para Vivir Mejor"
Puebla, Pue., a 14 de junio de 2021

DR. FELIPE PÉREZ RODRÍGUEZ
DIRECTOR

C.c.p. Archivo
DR*FPR/DR*AMB/*mhr

Instituto de Física
"Luis Rivera Terrazas"

Av. San Claudio esq. 18 Sur, Edif. IF1,
Ciudad Universitaria, Col. San Manuel
Puebla, Pue. C.P. 72570
01 (222) 229 55 00 Ext. 5610, 5611, 2008